Nuclear Science

ISBN 92-64-02330-5
NEA/NSC/DOC(2006)20

NEA Nuclear Science Committee
Working Party on Scientific Issues of Reactor Systems

PWR MOX/UO_2 Core Transient Benchmark

Final Report

January 2007

Tomasz Kozlowski
Purdue University, USA, and KTH, Sweden

Thomas J. Downar
Purdue University, USA

NEA No. 6048

NUCLEAR ENERGY AGENCY
ORGANISATION FOR ECONOMIC CO-OPERATION AND DEVELOPMENT
US NUCLEAR REGULATORY COMMISSION

ORGANISATION FOR ECONOMIC CO-OPERATION AND DEVELOPMENT

The OECD is a unique forum where the governments of 30 democracies work together to address the economic, social and environmental challenges of globalisation. The OECD is also at the forefront of efforts to understand and to help governments respond to new developments and concerns, such as corporate governance, the information economy and the challenges of an ageing population. The Organisation provides a setting where governments can compare policy experiences, seek answers to common problems, identify good practice and work to co-ordinate domestic and international policies.

The OECD member countries are: Australia, Austria, Belgium, Canada, the Czech Republic, Denmark, Finland, France, Germany, Greece, Hungary, Iceland, Ireland, Italy, Japan, Korea, Luxembourg, Mexico, the Netherlands, New Zealand, Norway, Poland, Portugal, the Slovak Republic, Spain, Sweden, Switzerland, Turkey, the United Kingdom and the United States. The Commission of the European Communities takes part in the work of the OECD.

OECD Publishing disseminates widely the results of the Organisation's statistics gathering and research on economic, social and environmental issues, as well as the conventions, guidelines and standards agreed by its members.

* * *

This work is published on the responsibility of the Secretary-General of the OECD. The opinions expressed and arguments employed herein do not necessarily reflect the official views of the Organisation or of the governments of its member countries.

NUCLEAR ENERGY AGENCY

The OECD Nuclear Energy Agency (NEA) was established on 1st February 1958 under the name of the OEEC European Nuclear Energy Agency. It received its present designation on 20th April 1972, when Japan became its first non-European full member. NEA membership today consists of 28 OECD member countries: Australia, Austria, Belgium, Canada, the Czech Republic, Denmark, Finland, France, Germany, Greece, Hungary, Iceland, Ireland, Italy, Japan, Luxembourg, Mexico, the Netherlands, Norway, Portugal, Republic of Korea, the Slovak Republic, Spain, Sweden, Switzerland, Turkey, the United Kingdom and the United States. The Commission of the European Communities also takes part in the work of the Agency.

The mission of the NEA is:

- to assist its member countries in maintaining and further developing, through international co-operation, the scientific, technological and legal bases required for a safe, environmentally friendly and economical use of nuclear energy for peaceful purposes, as well as
- to provide authoritative assessments and to forge common understandings on key issues, as input to government decisions on nuclear energy policy and to broader OECD policy analyses in areas such as energy and sustainable development.

Specific areas of competence of the NEA include safety and regulation of nuclear activities, radioactive waste management, radiological protection, nuclear science, economic and technical analyses of the nuclear fuel cycle, nuclear law and liability, and public information. The NEA Data Bank provides nuclear data and computer program services for participating countries.

In these and related tasks, the NEA works in close collaboration with the International Atomic Energy Agency in Vienna, with which it has a Co-operation Agreement, as well as with other international organisations in the nuclear field.

FOREWORD

The OECD/NEA Working Party on the Physics of Plutonium Fuels and Innovative Fuel Cycles (WPPR) was established in 1993 and reports to the OECD/NEA Nuclear Science Committee. Its main activity has been to analyse benchmarks carried out to answer technical questions related to the physics of plutonium fuels. Past volumes of published work have examined the physics of plutonium-fuelled pressurised water reactors (PWRs) and boiling water reactors (BWRs), as well as the physics of metal- and oxide-fuelled fast reactors. The present report concentrates on plutonium-fuelled, high-temperature reactors (HTRs). This activity was taken over and expanded by a new NEA Working Party on Scientific Issues in Reactor Systems (WPRS).

The present volume addresses a rod ejection transient in a core loaded partially with weapons-grade, mixed-oxide (MOX) fuel. The neutronics characteristics of plutonium are sufficiently different from uranium to significantly change the kinetics response of the reactor core. The reactor core chosen for the simulation is based on a four-loop Westinghouse PWR power plant similar to the reactor proposed for plutonium disposition in the United States. This is relevant to current international plutonium utilisation strategies as many of the commercial power plants in Europe and Japan already use MOX fuel and the United States is preparing to use MOX in light water reactors (LWRs) as part of its weapons plutonium disposition programme.

This work was sponsored by the US Nuclear Regulatory Commission (NRC) and the OECD Nuclear Energy Agency (NEA).

The *Physics of Plutonium Recycling* series currently comprises the following titles:

- Volume I: *Issues and Perspectives* (OECD/NEA, 1995).
- Volume II: *Plutonium Recycling in Pressurised Water Reactors* (OECD/NEA, 1995).
- Volume III: *Void Reactivity Effect in Pressurised Water Reactors* (OECD/NEA, 1995).
- Volume IV: *Fast Plutonium Burner Reactors: Beginning of Life* (OECD/NEA, 1995).
- Volume V: *Plutonium Recycling in Fast Reactors* (OECD/NEA, 1996).
- Volume VI: *Multiple Plutonium Recycling in Advanced PWRs* (OECD/NEA, 2002).
- Volume VII: *BWR MOX Benchmark – Specification and Results* (OECD/NEA, 2003).
- *Plutonium Management in the Medium Term – A Review by the OECD/NEA Working Group on the Physics of Plutonium Fuels and Innovative Systems (WPPR)* (OECD/NEA, 2003).

Acknowledgements

This benchmark is a result of over four years of effort in preparation and distribution of the specifications, and collection and analysis of the results. The benchmark organisers express their sincere gratitude to the participants who devoted their time and effort to this benchmark.

This work has been performed under the auspices of OECD/NEA Working Party on Scientific Issues of Reactor Systems (WPRS) and was sponsored by the US NRC and OECD/NEA.

TABLE OF CONTENTS

List of tables

List of figures

EXECUTIVE SUMMARY

The Nuclear Science Committee of the OECD Nuclear Energy Agency (NEA) has in the past organised a series of numerical and experimental benchmarks to verify the current level of accuracy in pin-power calculations and to identify the relative merits of various calculation methods. It is essential to accurately calculate the pin-power of a reactor core with a high degree of accuracy in order to make the correct decisions regarding the core design, burn-up cycle and safety margins. The present numerical benchmark was designed to provide the framework to assess the ability of modern reactor kinetics codes to predict the transient response of a core partially loaded with mixed-oxide (MOX) fuel to a control rod ejection transient.

The benchmark employs many of the characteristics of the NEACRP L-335 Pressurised Water Reactor (PWR) benchmark proposed by Finnemann in 1991 [1]. The current problem adds the complexity of modelling a control rod ejection in a core loaded partially with weapons-grade MOX since the neutronics characteristics of plutonium are sufficiently different than uranium to significantly change the kinetics response of the reactor core. The reactor core chosen for the simulation is based on four-loop Westinghouse PWR power plant similar to the reactor proposed for plutonium disposition in the USA. This is relevant to current international plutonium utilisation strategies as many of the commercial power plants in Europe and Japan already use MOX fuel and the USA is preparing to use MOX in light water reactors (LWRs) as part of its weapons plutonium disposition programme.

The benchmark participants used the latest versions of nuclear data sets and the most advanced core simulators. The methods varied from few-group nodal diffusion and multi-group heterogeneous transport calculations to continuous-energy Monte Carlo calculations of the heterogeneous core configuration.

All nodal diffusion codes were found to be capable of modelling the static MOX core, with only minor differences between results due to spatial discretisation, cross-sections interpolation and the pin-power reconstruction method. The relative difference compared to multi-group heterogeneous transport reference was found to be 1-2% relative assembly power distribution for the un-rodded state and 2-4% relative assembly power distribution for the heavily rodded state. Similar relative errors were found for static pin-power prediction.

All nodal diffusion codes were found to provide consistent results for the transient solution of the MOX core, with the only differences between results due to spatial and temporal discretisation, cross-section interpolation and the pin-power reconstruction method. A consistent comparison with a higher order transient method was not possible at the time of the preparation of the report because an appropriate heterogeneous solution method was not yet available.

Chapter 1

INTRODUCTION

Computational benchmarks based on a well defined problem with a complete set of input and a unique solution are often used as a means of verifying the reliability of numerical solutions. The problems usually employ some simplifications in order to make the analysis manageable and to enable the consistent comparison of several different models, yet complex enough to make the problem applicable to actual core designs.

The Nuclear Science Committee of the OECD Nuclear Energy Agency (NEA) has in the past organised a series of numerical and experimental benchmarks to verify the current level of accuracy in pin-power calculations and to identify the relative merits of various calculation methods. It is essential to accurately calculate the pin-power of a reactor core with a high degree of accuracy in order to make the correct decisions regarding the core design, burn-up cycle and safety margins. The present numerical benchmark was designed to provide the framework to assess the ability of modern reactor kinetic codes to predict the transient response of a core partially loaded with mixed-oxide (MOX) fuel to a control rod ejection transient.

The benchmark employs many of the characteristics of the NEACRP L-335 Pressurised Water Reactor (PWR) benchmark proposed by Finnemann in 1991 [1]. The current problem adds the complexity of modelling a control rod ejection in a core loaded partially with weapons-grade MOX since the neutronics characteristics of plutonium are sufficiently different than uranium to significantly change the kinetics response of the reactor core. The reactor core chosen for the simulation is based on four-loop Westinghouse PWR power plant similar to the reactor proposed for plutonium disposition in the USA. This is relevant to current international plutonium utilisation strategies as many of the commercial power plants in Europe and Japan already use MOX fuel and the USA is preparing to use MOX in light water reactors (LWRs) as part of its weapons plutonium disposition programme.

The rod ejection may occur in a PWR as a consequence of the rupture of the drive mechanism casing located on the reactor pressure vessel. This event is of particular concern for MOX-fuelled cores since the kinetics characteristics of plutonium are significantly different than uranium (e.g. the delayed neutron fraction of MOX fuel is significantly smaller than UO_2 cores, mainly due to high ^{239}Pu content). The rod ejection transient can result in significant, localised distortions of the neutron flux resulting in perturbations of the neutronic and thermal-hydraulic (T-H) core parameters which can be difficult for reactor core simulators to predict accurately, particularly in a heterogeneous MOX-fuelled core.

Nine participating groups provided twelve solutions using the latest versions of nuclear data sets and various advanced core simulation methods. Most solutions were submitted with the two-group nodal diffusion methods (the codes CORETRAN, EPISODE, NUREC, PARCS and SKETCH-INS). An additional multi-group nodal diffusion calculation was performed with PARCS and multi-group cell homogeneous transport solutions were performed with BARS and DORT. Cell heterogeneous transport calculations were performed with DeCART and MCNP using deterministic and stochastic solutions, respectively. This report provides a detailed comparison of the results of all the participants.

Chapter 2

BENCHMARK DESCRIPTION

The problem was designed primarily to assess core simulators, therefore, few-group constants were specified at the level of homogenised assembly and homogenised pin-cells. However, since some of the benchmark participants wished to utilise their own cross-section generation codes or were able to model explicitly the heterogeneous pins in their core simulators, the benchmark also specified material compositions and pin geometries. This is also useful for systematic evaluation of spatial homogenisation, energy condensation and angular approximations, although it was not a direct objective of the benchmark.

The core chosen for the simulation was based on four-loop Westinghouse PWR power plant similar to the reactor chosen for plutonium disposition in the USA. The problem geometry simulated here was a full PWR core at equilibrium cycle conditions in order to allow the realistic simulation of a single rod ejection. A quarter-core loading pattern is specified due to core symmetry and is shown in Figure 1.

Figure 1. Quarter-core loading pattern

	1	2	3	4	5	6	7	8
A	U 4.2% (CR-D) 35.0	U 4.2% 0.15	U 4.2% (CR-A) 22.5	U 4.5% 0.15	U 4.5% (CR-SD) 37.5	M 4.3% 17.5	U 4.5% (CR-C) 0.15	U 4.2% 32.5
B	U 4.2% 0.15	U 4.2% 17.5	U 4.5% 32.5	M 4.0% 22.5	U 4.2% 0.15	U 4.2% (CR-SB) 32.5	M 4.0% 0.15	U 4.5% 17.5
C	U 4.2% (CR-A) 22.5	U 4.5% 32.5	U 4.2% (CR-C) 22.5	U 4.2% 0.15	U 4.2% 22.5	M 4.3% 17.5	U 4.5% (CR-B) 0.15	M 4.3% 35.0
D	U 4.5% 0.15	M 4.0% 22.5	U 4.2% 0.15	M 4.0% 37.5	U 4.2% 0.15	U 4.5% (CR-SC) 20.0	M 4.3% 0.15	U 4.5% 20.0
E	U 4.5% (CR-SD) 37.5	U 4.2% 0.15	U 4.2% 22.5	U 4.2% 0.15	U 4.2% (CR-D) 37.5	U 4.5% 0.15	U 4.2% (CR-SA) 17.5	
F	M 4.3% 17.5	U 4.2% (CR-SB) 32.5	M 4.3% 17.5	U 4.5% (CR-SC) 20.0	U 4.5% 0.15	M 4.3% 0.15	U 4.5% 32.5	
G	U 4.5% (CR-C) 0.15	M 4.0% 0.15	U 4.5% (CR-B) 0.15	M 4.3% 0.15	U 4.2% (CR-SA) 17.5	U 4.5% 32.5	Assembly Type CR Position Burnup [GWd/t]	
H	U 4.2% 32.5	U 4.5% 17.5	M 4.3% 35.0	U 4.5% 20.0			Fresh Once Burn Twice Burn	

CR-A	Control Rod Bank A
CR-B	Control Rod Bank B
CR-C	Control Rod Bank C
CR-D	Control Rod Bank D
CR-SA	Shutdown Rod Bank A
CR-SB	Shutdown Rod Bank B
CR-SC	Shutdown Rod Bank C
CR-SD	Shutdown Rod Bank D
O	Ejected Rod

The core was designed based on the following reasonable, but not necessary, guidelines proposed for cores partially loaded with MOX fuel:

- no fresh MOX on the core periphery;
- no MOX assemblies facing each other;
- no MOX assemblies in control rod position;
- maximum 1/3 of the core loaded with MOX fuel;
- no integral fuel burnable absorbers (IFBA) in MOX assemblies;
- a three-batch equilibrium cycle.

The objective of the benchmark problem was to evaluate core simulators through a sequence of calculations. Calculations were divided into four parts:

- Part I, 2-D fixed T-H conditions – calculate multiplication factor, rod worth, assembly and pin power;
- Part II, 3-D hot full power (HFP) conditions – calculate critical boron concentration, assembly and pin power;
- Part III, 3-D hot zero power (HZP) conditions – calculate critical boron concentration, assembly and pin power;
- Part IV, 3-D with Part III conditions – calculate transient response to control rod ejection accident.

A complete description of the benchmark problem, including all necessary details and description of modelling simplifications and assumptions, is given in Appendix A. Included in the specifications are all geometry, material and feedback data required to develop the detailed three-dimensional computational model of the full core reactor at any homogenisation level desired – nodal (assembly homogenised), pin-by-pin (pin cell homogenised) or heterogeneous. Apart from the geometry and material data, the isotopic concentrations of each medium were also provided in separate data files to eliminate any discrepancies between participants using heterogeneous models. Separate data files were also provided for the nodal cross-sections, pin-by-pin cross-sections and submittal templates.

Nodal and pin-by-pin homogeneous cross-sections were generated using HELIOS 1.7 with a 47-group library. Since the DeCART neutron library is based on the same 47-group library, DeCART was used as a reference whenever possible. This results in the most consistent comparison possible between multi-group heterogeneous transport methods and few-group nodal diffusion methods.

Chapter 3

PARTICIPANTS, CODES AND DATA

Nine participating groups provided twelve solutions to the benchmark. Eight solutions were obtained using the nodal diffusion method with the codes CORETRAN, EPISODE, NUREC, PARCS and SKETCH-INS, seven of which were two-group (2G) and two were multi-group (MG). For the heterogeneous transport solutions, two were obtained using the cell homogeneous method with the codes BARS and DORT and two were obtained using the full core heterogeneous method with the codes DeCART and MCNP.

The complete list of participants, codes, methods and cross-section libraries used is presented below. A summary of submitted solutions is shown in Table 1. Calculation details provided by the participants can be found in Appendix B.

Nodal (assembly homogeneous) solutions

1. **PSI, Switzerland**
   Participants:Hakim Ferroukhi, Martin Zimmermann
   Code: CORETRAN
   Method: 2G nodal diffusion
   Cross-sections: Benchmark provided 2G nodal library

2. **Osaka University, Japan**
   Participants: Toshikazu Takeda, Sho Tanaka
   Code: EPISODE
   Method: 2G nodal diffusion
   Cross-sections: Benchmark provided 2G nodal library

3. **KAERI, Korea**
   Participants: Hyun Chul Lee, Jae Woon Yoo, Jae Man Noh, Hyung Kook Joo
   Code: NUREC
   Method: 2G nodal diffusion
   Cross-sections: Benchmark provided 2G nodal library

4. **Purdue University, USA**
   Participants: Tomasz Kozlowski, Thomas J. Downar
   Code: PARCS
   Method: 2G and MG nodal diffusion
   Cross-sections: Benchmark provided 2G, 4G and 8G nodal library

5. **JNES, Japan**
   Participants: Akiko Takeuchi, Tetsuo Nakajima
   Code: SKETCH-INS
   Method: 2G nodal diffusion
   Cross-sections: Benchmark provided 2G nodal library

Heterogeneous (cell homogeneous or cell heterogeneous) solutions

6. **Kurchatov Institute, Russia**
   Participants: Sergey Akimushkin, Alexander Avvakumov, Valery Malofeev, Victor Sidorov
   Code: BARS
   Method: MG cell homogeneous lambda matrix
   Cross-sections: UNK generated 5G library using benchmark provided isotopic compositions

7. **Seoul National University/KAERI, Korea**
   Participants: Han-Gyu Joo, Jin-Young Cho, Kang-Seog Kim
   Code: DeCART
   Method: MG cell heterogeneous MOC transport
   Cross-sections: Heterogeneous 47G library based on HELIOS

8. **GRS, Germany**
   Participants: Armin Seubert, Winfried Zwermann, Siegfried Langenbuch
   Code: DORT
   Method: MG cell homogeneous S_N transport
   Cross-sections: HELIOS generated 16G library using benchmark provided isotopic compositions

9. **Kurchatov Institute, Russia**
   Participants: Andrey Myasnikov
   Code: MCNP
   Method: Continuous-energy cell heterogeneous Monte Carlo transport
   Cross-sections: ENDF/B-VI, processed with NJOY

Table 1. Participants, codes and data libraries

Nodal solutions				
Code (solution type)	**Organisation (country)**	**Solution method**	**Groups/ homogenisation**	**Cross-section library**
CORETRAN 1/FA*	PSI (Switzerland)	Nodal diffusion	2G Nodal	2G benchmark library
CORETRAN 4/FA*	PSI (Switzerland)	Nodal diffusion	2G Nodal	2G benchmark library
EPISODE	Osaka Univ. (Japan)	Nodal diffusion	2G Nodal	2G benchmark library
NUREC	KAERI (Korea)	Nodal diffusion	2G Nodal	2G benchmark library
PARCS 2G	Purdue Univ. (USA)	Nodal diffusion	2G Nodal	2G benchmark library
PARCS 4G	Purdue Univ. (USA)	Nodal diffusion	4G Nodal	4G benchmark library
PARCS 8G	Purdue Univ. (USA)	Nodal diffusion	8G Nodal	8G benchmark library
SKETCH-INS	JNES (Japan)	Nodal diffusion	2G Nodal	2G benchmark library
Heterogeneous solutions				
BARS	Kurchatov Inst. (Russia)	Lambda matrix	5G Cell hom	UNK generated
DeCART	SNU/KAERI (Korea)	MOC	47G Cell het	HELIOS based
DORT	GRS (Germany)	S_N	16G Cell hom	HELIOS generated
MCNP	Kurchatov Inst. (Russia)	Monte Carlo	Continuous Cell het	ENDF/B-VI with NJOY

* 1/FA or 4/FA means 1 or 4 node(s) per fuel assembly.

Chapter 4

BENCHMARK RESULTS

The summary of all submitted results is shown in Table 2. A detailed submittal checklist with a complete list of requested information is a part of the benchmark specifications and is included in Appendix A.

Only the nodal codes were developed well enough to be able to provide all requested edit information. In most cases, the missing data are only a reflection of particular code output options rather than its simulation capabilities. From the high-order multi-group heterogeneous transport solutions, only BARS and DeCART have feedback and transient capabilities, although some current programming limitations prevented DeCART from providing transient solution. The transport codes without feedback and transient capability, DORT and MCNP, were able to perform only Part I of the benchmark. Calculation details provided by the participants can be found in Appendix B.

In order to accurately describe error distribution, the two metrics used for comparison of the results were power-weighted error (PWE) and error-weighted error (EWE). Both are defined as a weighted average of the error by Eq. (1) and Eq. (2), respectively. The PWE is similar to absolute error. It weights the per cent error with the reference power, therefore the PWE diminishes the importance of error in the low power region and amplifies error in the high power region. The EWE is similar to RMS error. It weights the largest per cent errors more than the small ones and is not linked to the actual power distribution. Therefore, it can report artificially large error, such as when only low power assembly or pin locations are predicted poorly.

$$PWE = \frac{\sum_i |e_i| ref_i}{\sum_i ref_i} \tag{1}$$

$$EWE = \frac{\sum_i |e_i| |e_i|}{\sum_i |e_i|} \tag{2}$$

where:

$$e_i = \frac{calc_i - ref_i}{ref_i} \times 100 \tag{3}$$

Table 2. Summary of submitted results

	CORETRAN 1/FA	CORETRAN 4/FA	EPISODE	NUREC	PARCS 2G	PARCS 4G	PARCS 8G	SKETCH-INS	BARS	DeCART	DORT	MCNP
Part I, 2-D fixed T-H												
Multiplication factor	Y	Y	Y	Y	Y	Y	Y	Y	Y	Y	P	Y
Radial assembly power	Y	Y	Y	Y	Y	Y	Y	Y	Y	Y	P	Y
Radial pin power	Y	–	Y	Y	Y	–	–	Y	Y	Y	P	–
Rod worth	Y	Y	Y	Y	Y	Y	Y	Y	Y	–	–	–
Part II, 3-D hot full power												
Critical boron concentration	Y	Y	Y	Y	Y	Y	Y	Y	–	–	–	–
Radial assembly power	Y	Y	Y	Y	Y	Y	Y	Y	–	–	–	–
Radial pin power	Y	–	Y	Y	Y	–	–	Y	–	–	–	–
Radial T-H conditions	Y	Y	Y	Y	Y	Y	Y	Y	–	–	–	–
Axial power	Y	Y	Y	Y	Y	Y	Y	Y	–	–	–	–
Axial T-H conditions	Y	Y	Y	Y	Y	Y	Y	Y	–	–	–	–
Part III, 3-D hot zero power												
Critical boron concentration	Y	Y	Y	Y	Y	Y	Y	Y	Y	Y	–	–
Core delayed neutron fraction	Y	Y	Y	Y	Y	Y	Y	Y	Y	–	–	–
Radial assembly power	Y	Y	Y	Y	Y	Y	Y	Y	Y	Y	–	–
Radial pin power	Y	–	Y	Y	Y	–	–	Y	Y	Y	–	–
Axial power	Y	Y	Y	Y	Y	Y	Y	Y	Y	Y	–	–
Part IV, 3-D transient												
Transient core power	Y	Y	Y	Y	Y	Y	Y	Y	Y	–	–	–
Transient reactivity	Y	Y	Y	–	Y	Y	Y	Y	Y	–	–	–
Transient peaking factors	Y	P	–	Y	Y	P	P	Y	Y	–	–	–
Transient T-H conditions	Y	Y	Y	Y	Y	Y	Y	Y	Y	–	–	–
Snapshot radial assembly power	Y	Y	Y	Y	Y	Y	Y	Y	Y	–	–	–
Snapshot radial pin power	Y	–	Y	Y	Y	–	–	Y	Y	–	–	–
Snapshot axial power	Y	Y	Y	Y	Y	Y	Y	Y	Y	–	–	–
Snapshot axial T-H conditions	Y	Y	Y	Y	Y	Y	Y	Y	Y	–	–	–

Y – yes, complete data provided.
P – partial data provided.
– – no data provided.

4.1 Comparison of Part I – 2-D fixed T-H conditions

All of the benchmark participants submitted a solution for Part I of the benchmark. The DeCART solution was used as a reference for purposes of comparing assembly and pin-power distributions. The reference assembly power density is shown in Figure 2 and Figure 3 at all rods out (ARO) and all rods in (ARI) conditions, respectively.

Figure 2. Part I, reference assembly power density at ARO

	1	2	3	4	5	6	7	8
A	1.374	1.735	1.418	1.525	1.035	1.032	0.997	0.413
B	1.735	1.563	1.245	1.277	1.349	0.918	0.978	0.491
C	1.418	1.245	1.325	1.446	1.247	1.114	0.991	0.393
D	1.525	1.277	1.446	1.076	1.308	1.143	0.892	0.341
E	1.035	1.348	1.247	1.308	0.904	1.067	0.585	
F	1.032	0.917	1.114	1.142	1.067	0.754	0.281	
G	0.997	0.978	0.991	0.892	0.585	0.281		
H	0.413	0.491	0.393	0.340				

Figure 3. Part I, reference assembly power density at ARI

	1	2	3	4	5	6	7	8
A	1.209	2.533	1.202	2.196	0.742	0.669	0.300	0.205
B	2.533	2.459	1.812	2.103	1.832	0.449	0.489	0.268
C	1.202	1.812	1.198	2.452	1.944	0.985	0.329	0.198
D	2.196	2.103	2.452	1.823	1.675	0.531	0.450	0.186
E	0.742	1.832	1.944	1.675	0.508	0.696	0.190	
F	0.669	0.449	0.985	0.531	0.696	0.562	0.186	
G	0.300	0.489	0.329	0.450	0.190	0.186		
H	0.205	0.268	0.198	0.186				

Table 3 shows a comparison of eigenvalues and assembly-wise power. At ARO conditions all heterogeneous solutions are in a very good agreement, however, at ARI, there are differences in the BARS solution. As evident from the large difference between %PWE and %EWE, the reason for the large difference is the power prediction in low power regions at the core periphery and control rod locations. The heavily rodded condition is very difficult for any code to predict, and closer investigation revealed that library differences were the reason for consistently lower rod worth predictions resulting in differences in the power distribution and a different radial leakage because of the differences in the peripheral power.

Table 3. Part I, comparison of eigenvalues and assembly power

	Eigenvalue		Todal Rod Worth	Assembly Power Error			
				ARO		ARI	
	ARO	ARI	[dk/k]	%PWE	%EWE	%PWE	%EWE
nodal							
CORETRAN 1/FA	1.06387	0.99202	6808	1.06	1.69	2.01	2.52
CORETRAN 4/FA	1.06379	0.99154	6850	0.96	1.64	1.67	2.18
EPISODE	1.06364	0.99142	6849	0.96	1.64	1.66	2.16
NUREC	1.06378	0.99153	6850	0.96	1.63	1.64	2.16
PARCS 2G	1.06379	0.99154	6850	0.96	1.63	1.67	2.18
PARCS 4G	1.06376	0.99136	6865	0.90	1.42	1.61	2.26
PARCS 8G	1.06354	0.99114	6868	0.86	1.25	1.65	2.49
SKETCH-INS	1.06379	0.99153	6850	0.97	1.67	1.67	2.16
heterogeneous							
BARS	1.05826	0.98775	6745	1.29	1.92	3.92	10.30
DeCART	1.05852	0.98743	6801	ref	ref	ref	ref
DORT	1.06036	-	-	0.86	1.12	-	-
MCNP	1.05699	0.98540	6873	0.67	1.26	1.33	3.67

The agreement between nodal methods is excellent, with the only difference due to the spatial discretisation used by each code. The cross-section interpolation error was not a factor since the cross-sections were provided exactly at the fixed T-H conditions and required no interpolation. The agreement between DeCART and the nodal methods is very good even at ARI conditions, giving additional confidence in nodal cross-sections and the homogenisation process.

One of the interesting results is the absence of any significant difference in the two-group versus multi-group solutions. Even with the MOX assembly plutonium content being almost as high as the ^{235}U enrichment in the UO_2 assemblies, the group effect is not significant for this problem. The 2G, 4G and 8G nodal solutions are very similar. At ARO the increasing number of groups improves the results only slightly, whereas at ARI no improvement is observed and there is even a slight increase in %EWE. Most likely, this is because of competing effects of group and spatial discretisation. Even though the 8G solution should have a lower energy discretisation error, it also has a larger spatial discretisation error because of a more complicated spatial shape of the neutron flux. This is especially true in the low energy groups where the group-to-group interactions are more significant. Multi-group NEM with four nodes per fuel assembly (4/FA) as used in PARCS solution may not be sufficient since both the spatial distribution within the node and leakage distribution on the assembly interface is more complicated and requires appropriate spatial resolution.

The difference between the highest and the lowest total rod worth prediction is only 128 pcm, with the highest and the lowest prediction given by MCNP and BARS, respectively. Given the differences between methods and neutron libraries, this is reasonably good agreement. Other than these two results, the difference decreases to only 66 pcm.

The single rod worth at ARO and ARI conditions are shown in Tables 4 and 5, respectively. The only heterogeneous solution available is from BARS.

Table 4. Part I, rod worth at ARO [dk/k]

	Rod Position									
	(A,1)	(A,3)	(A,5)	(A,7)	(B,6)	(C,3)	(C,7)	(D,6)	(E,5)	(E,7)
nodal										
CORETRAN 1/FA	164	143	91	53	70	122	51	68	64	28
CORETRAN 4/FA	166	144	92	53	70	123	51	69	65	28
EPISODE	165	134	-	53	70	123	51	69	64	27
NUREC	166	143	91	53	70	122	51	68	64	27
PARCS 2G	166	143	91	53	70	123	51	68	64	27
PARCS 4G	167	144	91	53	70	122	51	68	64	27
PARCS 8G	168	144	91	52	69	123	50	68	64	27
SKETCH-INS	166	143	91	53	70	123	51	68	64	27
heterogeneous										
BARS	166	139	87	49	66	117	49	66	63	27
DeCART	-	-	-	-	-	-	-	-	-	-
DORT	-	-	-	-	-	-	-	-	-	-
MCNP	-	-	-	-	-	-	-	-	-	-

Table 5. Part I, rod worth at ARI [dk/k]

	Rod Position									
	(A,1)	(A,3)	(A,5)	(A,7)	(B,6)	(C,3)	(C,7)	(D,6)	(E,5)	(E,7)
nodal										
CORETRAN 1/FA	-826	-875	-397	-57	-151	-1115	-78	-291	-246	-22
CORETRAN 4/FA	-840	-880	-405	-55	-152	-1127	-78	-290	-249	-20
EPISODE	-843	-884	-	-59	-155	-1130	-81	-293	-253	-24
NUREC	-840	-880	-405	-56	-152	-1127	-78	-290	-249	-21
PARCS 2G	-840	-880	-405	-56	-152	-1127	-78	-290	-249	-21
PARCS 4G	-849	-886	-407	-55	-153	-1134	-77	-290	-250	-21
PARCS 8G	-857	-889	-409	-54	-153	-1139	-76	-290	-253	-20
SKETCH-INS	-840	-880	-405	-56	-152	-1127	-78	-290	-249	-21
heterogeneous										
BARS	-914	-921	-417	-44	-145	-1193	-68	-313	-268	-17
DeCART	-	-	-	-	-	-	-	-	-	-
DORT	-	-	-	-	-	-	-	-	-	-
MCNP	-	-	-	-	-	-	-	-	-	-

At ARO the agreement between the nodal solutions and heterogeneous BARS solution is very good, with the BARS rod worth being slightly lower. The maximum difference between the highest and the lowest rod prediction is only 10 pcm and occurs at position (A,3).

At ARI the agreement between the nodal solutions and the BARS solution is not as good but is still reasonable. The maximum difference between the highest and the lowest rod prediction is 88 pcm and occurs at position (A,1). All other positions have significantly higher differences between the nodal and the BARS solution than at ARO, as well. However, it is no longer possible to see that the BARS rod worth is consistently lower than the nodal solutions. This is because the power shape at ARI is very different between the nodal and the BARS solution, causing a difference in rod worth that can be positive or negative.

A comparison of pin-power at the ARO state is shown in Tables 6 and 7, and a comparison of pin power at the ARI state is shown in Tables 8 and 9. Even though the eigenvalue and the assembly power were almost identical between the nodal codes, the pin power reveals significant differences between the pin-power reconstruction methods used in each code. In particular, CORETRAN is noticeably different than the other nodal codes' pin-power prediction. This is because CORETRAN does not use the corner balance equation for the homogeneous flux shape calculation and its definition of corner discontinuity factors is not the true heterogeneous to homogeneous corner point flux ratio.

Table 6. Part I, pin power %PWE at ARO

	Assembly Position					
	(A,1)	(B,2)	(C,3)	(D,4)	(E,5)	(F,6)
nodal						
CORETRAN 1/FA	0.85	1.05	0.91	2.37	1.38	4.89
CORETRAN 4/FA	-	-	-	-	-	-
EPISODE	0.25	0.23	0.42	1.37	0.47	4.04
NUREC	0.24	0.22	0.31	0.67	0.32	0.87
PARCS 2G	0.28	0.21	0.29	0.54	0.32	0.51
PARCS 4G	-	-	-	-	-	-
PARCS 8G	-	-	-	-	-	-
SKETCH-INS	0.22	0.22	0.32	0.71	0.32	1.05
heterogeneous						
BARS	0.26	0.45	0.55	0.40	0.33	0.61
DeCART	ref	ref	ref	ref	ref	ref
DORT	1.52	0.59	0.92	0.33	1.64	0.41
MCNP	-	-	-	-	-	-

Table 7. Part I, pin power %EWE at ARO

	Assemby Position					
	(A,1)	(B,2)	(C,3)	(D,4)	(E,5)	(F,6)
nodal						
CORETRAN 1/FA	1.32	1.65	1.93	5.00	2.63	8.66
CORETRAN 4/FA	-	-	-	-	-	-
EPISODE	0.55	0.47	0.71	3.47	0.94	7.83
NUREC	0.48	0.46	0.43	1.17	0.68	1.96
PARCS 2G	0.54	0.45	0.41	0.79	0.60	1.05
PARCS 4G	-	-	-	-	-	-
PARCS 8G	-	-	-	-	-	-
SKETCH-INS	0.44	0.44	0.49	1.63	0.58	2.89
heterogeneous						
BARS	0.34	0.66	0.83	0.58	0.52	1.13
DeCART	ref	ref	ref	ref	ref	ref
DORT	1.63	0.71	1.13	0.48	1.77	0.67
MCNP	-	-	-	-	-	-

Table 8. Part I, pin power %PWE at ARI

	Assembly Position					
	(A,1)	(B,2)	(C,3)	(D,4)	(E,5)	(F,6)
nodal						
CORETRAN 1/FA	6.22	1.31	5.95	3.26	7.75	3.99
CORETRAN 4/FA	-	-	-	-	-	-
EPISODE	2.44	0.28	2.32	1.35	2.37	3.83
NUREC	-	0.33	-	0.66	-	0.77
PARCS 2G	-	0.63	-	0.65	-	0.50
PARCS 4G	-	-	-	-	-	-
PARCS 8G	-	-	-	-	-	-
SKETCH-INS	2.63	0.33	2.67	0.79	2.97	1.19
heterogeneous						
BARS	0.42	0.30	1.55	0.33	1.96	0.66
DeCART	ref	ref	ref	ref	ref	ref
DORT	-	-	-	-	-	-
MCNP	-	-	-	-	-	-

Table 9. Part I, pin power %EWE at ARI

	Assembly Position					
	(A,1)	(B,2)	(C,3)	(D,4)	(E,5)	(F,6)
nodal						
CORETRAN 1/FA	8.60	2.12	8.82	7.55	11.74	8.02
CORETRAN 4/FA	-	-	-	-	-	-
EPISODE	5.19	0.63	5.05	3.39	4.89	7.65
NUREC	-	0.59	-	1.10	-	1.72
PARCS 2G	-	1.61	-	1.43	-	1.12
PARCS 4G	-	-	-	-	-	-
PARCS 8G	-	-	-	-	-	-
SKETCH-INS	4.29	0.66	4.24	1.79	4.64	3.02
heterogeneous						
BARS	0.82	0.39	2.11	0.56	2.78	1.07
DeCART	ref	ref	ref	ref	ref	ref
DORT	-	-	-	-	-	-
MCNP	-	-	-	-	-	-

Excluding CORETRAN results, all nodal codes consistently predict un-rodded UO_2 assemblies within fraction of a per cent, closely followed by MOX assemblies. The peripheral and rodded assemblies are the most difficult to predict, although because of their low power they are not as important as high-power assemblies where the peak power pin is most likely to occur. EPISODE has a very large error in the peripheral assembly, because it does not use the corner discontinuity factor on the reflector side of the peripheral fuel assembly, which is required for proper corner point balance.

Overall, the most challenging regions to predict by nodal codes' pin-power reconstruction methods are MOX, peripheral and rodded assemblies. This is because the space-energy separation assumption used by pin-power reconstruction methods is least applicable in these locations and therefore the accuracy of the homogenisation/de-homogenisation process is most challenged.

The difference in the pin-power prediction between different assembly types or their location is not as visible in the heterogeneous methods. They perform about as well for the UO_2, MOX and peripheral assemblies. The pin power calculated for a rodded assembly by a heterogeneous method can be compared only with BARS, which shows only a modest increase in the pin-power error and is still significantly better than nodal methods. This is surprising given the neutron library and rod worth prediction difference noted earlier. In general, nodal methods give as good a pin-power prediction as heterogeneous methods at the ARO state, but are significantly less accurate at the ARI state, especially at rodded locations.

4.2 Comparison of Part II – 3-D hot full power conditions

Only nodal solutions were submitted for Part II of the benchmark. Because of this, the PARCS 2G solution was used as the basis of comparison for assembly and pin-power distributions. The reference assembly power density is shown in Figure 4.

Figure 4. Part II, reference assembly power density

	1	2	3	4	5	6	7	8
A	1.092	1.370	1.187	1.367	1.014	1.117	1.118	0.486
B	1.370	1.252	1.070	1.197	1.301	0.973	1.115	0.580
C	1.187	1.070	1.169	1.334	1.209	1.192	1.112	0.485
D	1.367	1.197	1.334	1.066	1.289	1.180	1.006	0.402
E	1.014	1.301	1.209	1.289	0.932	1.123	0.645	
F	1.117	0.973	1.192	1.180	1.123	0.841	0.319	
G	1.118	1.115	1.112	1.006	0.645	0.319		
H	0.486	0.580	0.485	0.402				

A comparison of critical boron concentration, assembly power and core average T-H properties is shown in Table 10. The differences in the results can be attributed to differences in spatial discretisation, T-H calculation and cross-section interpolation. Since results are very close among all participants, this gives confidence that the feedback and cross-section interpolation were properly implemented. The difference between the highest and the lowest critical boron concentration is only 39 ppm.

Table 10. Part II, comparison of critical boron concentration, assembly power and core average T-H properties

	Critical Boron Concent. [ppm]	Assembly Power Error		Core Average T/H Properties				
		%PWE	%EWE	Doppler Temp. [K]	Moderator Density [kg/m3]	Moderator Temp. [K]	Outlet Mod. Density [kg/m3]	Outlet Mod. Temp. [K]
nodal								
CORETRAN 1/FA	1647	0.31	0.51	908.4	706.1	581.0	658.5	598.6
CORETRAN 4/FA	1645	0.26	0.46	908.4	706.1	581.0	658.5	598.6
EPISODE	1661	0.40	0.64	846.5	701.8	582.6	697.4	585.5
NUREC	1683	0.31	0.44	827.8	706.1	581.1	661.5	598.7
PARCS 2G	1679	ref	ref	836.0	706.1	581.3	662.1	598.8
PARCS 4G	1674	0.31	0.50	836.1	706.1	581.3	662.1	598.8
PARCS 8G	1672	0.55	0.86	836.2	706.1	581.3	662.1	598.8
SKETCH-INS	1675	1.04	1.39	836.6	705.5	580.9	659.6	598.9

EPISODE used feedback with cross-section interpolation in fuel temperature and moderator density performed without the use of cross terms. However, this did not appear to affect the results significantly since the critical boron concentration, radial power and axial power profile are consistent with other nodal solutions. This indicates that the cross-section cross terms are not very important for this problem.

EPISODE moderator properties stand out from the rest, although they do not seem to influence other results – critical boron concentration, radial or axial power distribution. This is especially surprising given that of all results its core average moderator density is the lowest and the outlet moderator density is the highest. Considering that the difference between core average and outlet moderator density and temperature is significantly lower than all other submitted results and that the radial and axial power distribution is still consistent with other results, it is possible that a typographical error was made in the submitted core average T-H properties.

The CORETRAN Doppler temperature is higher than that of other participants. This causes the critical boron concentration to be the lowest of all submitted results.

A comparison of pin-power distributions is shown in Tables 11 and 12. NUREC, PARCS and SKETCH-INS clearly use the same or very similar pin-power reconstruction method, whereas CORETRAN and EPISODE use different methods.

Table 11. Part II, pin power %PWE

	Assembly Position					
	(A,1)	(B,2)	(C,3)	(D,4)	(E,5)	(F,6)
nodal						
CORETRAN 1/FA	1.07	0.92	0.90	2.62	1.38	4.60
CORETRAN 4/FA	-	-	-	-	-	-
EPISODE	3.08	2.67	3.01	3.47	3.44	10.47
NUREC	0.08	0.17	0.24	0.32	0.13	0.89
PARCS 2G	ref	ref	ref	ref	ref	ref
PARCS 4G	-	-	-	-	-	-
PARCS 8G	-	-	-	-	-	-
SKETCH-INS	0.09	0.11	0.18	0.58	0.22	0.87

Table 12. Part II, pin power %EWE

	Assembly Position					
	(A,1)	(B,2)	(C,3)	(D,4)	(E,5)	(F,6)
nodal						
CORETRAN 1/FA	1.61	1.70	1.85	5.52	2.66	8.24
CORETRAN 4/FA	-	-	-	-	-	-
EPISODE	4.12	3.63	4.29	5.06	4.75	13.85
NUREC	0.15	0.25	0.40	1.10	0.32	1.56
PARCS 2G	ref	ref	ref	ref	ref	ref
PARCS 4G	-	-	-	-	-	-
PARCS 8G	-	-	-	-	-	-
SKETCH-INS	0.24	0.20	0.33	1.38	0.41	2.38

Since this is a code-to-code comparison with the same type of solution method, there should be no significant difference in the pin-power error between different assembly types or location. However, there is a significant increase in the pin-power error on the core periphery. This is due to the particular implementation of the pin-power reconstruction method and the other sources of error described earlier – spatial discretisation, T-H feedback and cross-section interpolation.

Axial power distribution is shown in Figure 5 and axial power distribution error is shown in Figure 6. The results reflect the combined effect of different sources of error described earlier in this section. In general, despite these differences, all results are consistent with each other and are within 2% away from the fuel-reflector interface. This gives additional confidence that the feedback and cross-section interpolations were properly implemented.

4.3 Comparison of Part III – 3-D hot zero power conditions

Solutions were submitted for Part III of the benchmark by all of the nodal and two of the heterogeneous codes, BARS and DeCART. The DeCART solution was used as a reference for assembly and pin-power comparisons. The reference assembly power density is shown in Figure 7.

Figure 5. Part II, axial power distribution

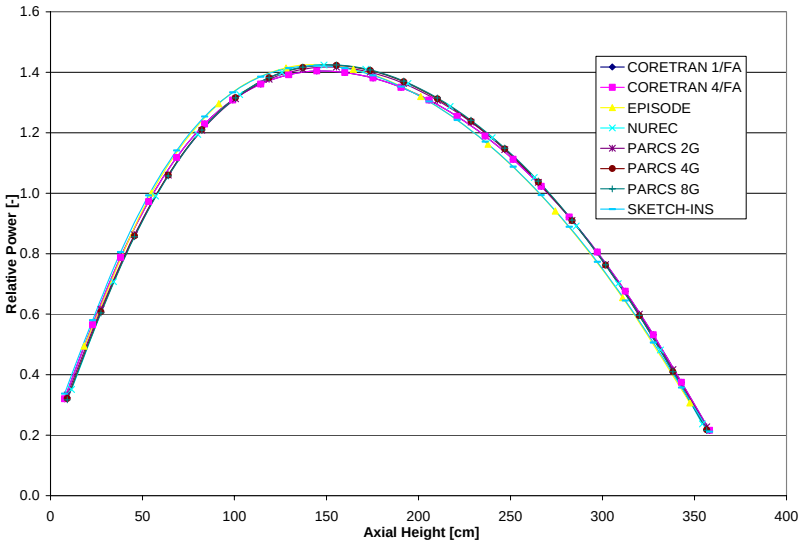

Figure 6. Part II, axial power distribution error

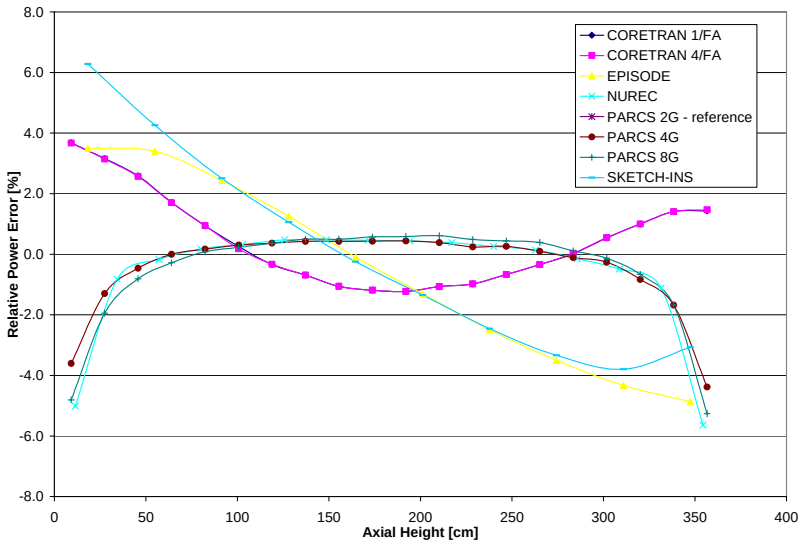

Figure 7. Part III, reference assembly power density

	1	2	3	4	5	6	7	8
A	0.385	0.847	0.542	1.510	1.296	1.160	0.496	0.293
B	0.847	0.871	0.823	1.357	1.733	1.073	0.831	0.392
C	0.542	0.823	0.633	1.563	1.631	1.342	0.557	0.324
D	1.510	1.357	1.563	1.297	1.615	1.462	1.050	0.373
E	1.296	1.733	1.631	1.615	0.633	1.367	0.824	
F	1.160	1.073	1.342	1.462	1.367	1.089	0.427	
G	0.496	0.831	0.557	1.050	0.824	0.427		
H	0.293	0.392	0.324	0.373				

A comparison of critical boron concentration, delayed neutron fraction and assembly power is shown in Table 13. The agreement between all results is very good with the assembly power error only slightly larger than for the 2-D problem in Part I of the benchmark. The agreement between nodal methods is excellent, with the only difference due to spatial discretisation. The cross-section interpolation error should be negligible at HZP conditions for this problem.

Table 13. Part III, comparison of critical boron concentration, delayed neutron fraction and assembly power

	Critical Boron Concent. [ppm]	Delayed Neutron Fraction [pcm]	Assembly Power Error	
			%PWE	%EWE
nodal				
CORETRAN 1/FA	1351	568	1.26	4.10
CORETRAN 4/FA	1346	568	1.09	3.72
EPISODE	1340	579	1.05	3.42
NUREC	1343	576	1.05	3.43
PARCS 2G	1341	579	1.05	3.49
PARCS 4G	1337	579	1.11	3.06
PARCS 8G	1334	580	1.20	2.85
SKETCH-INS	1341	579	1.06	3.77
heterogeneous				
BARS	1296	579	2.65	5.66
DeCART	1265	-	ref	ref

The difference between the highest and the lowest critical boron concentration is 86 ppm. However, it can be noted that the nodal solutions and the heterogeneous solutions fall into two distinct groups. The difference between all nodal solutions is only 17 ppm.

The delayed neutron fraction is in very good agreement as well, although the CORETRAN result is slightly lower. This is because CORETRAN does not use adjoint weighting of the delayed neutron fraction when calculating a single core-average value. It should be noted that even though the core-average value might be different, it is of no consequence for the kinetic calculation since the node-wise delayed neutron fraction is used in the calculation.

The slightly higher boron concentration predicted by CORETRAN appears to be attributable to a small difference in steam tables. Because of the small magnitude of the difference this effect is difficult to notice and identify, but it becomes apparent when considering results presented in Section 4.4.

Pin-power comparisons are shown in Tables 14 and 15. The general trends and the results are very similar to the pin-power results presented in Section 4.1, and the discussion used there is applicable for this section as well. It is worthwhile to note that the pin-power reconstruction works for the 3-D problems as well as it does for the 2-D problems.

Axial power distribution is shown in Figure 8 and axial power distribution error is shown in Figure 9. All results, except BARS, are in a good agreement. The BARS results are noticeably different, which indicates that its axial reflector model is significantly different than the one used by DeCART and nodal codes. The source of this discrepancy was found to be the differences in the neutron cross-section library. Similarly to axial power shape in Part II of the benchmark, all other results are consistent with each other and are within 2% away from the fuel-reflector interface. However, the error increases to about 10% close to the axial reflector. This can be expected for multi-group heterogeneous transport to few-group nodal diffusion difference close to the fuel-reflector interface and is not severe considering that it is a low power region. BARS axial power error was not plotted in Figure 9 because of significantly different scale.

Table 14. Part III, pin power %PWE

	Assembly Position					
	(A,1)	(B,2)	(C,3)	(D,4)	(E,5)	(F,6)
nodal						
CORETRAN 1/FA	6.46	0.81	6.66	3.44	6.71	4.81
CORETRAN 4/FA	-	-	-	-	-	-
EPISODE	2.51	0.57	2.33	1.41	2.39	3.88
NUREC	2.38	0.68	2.14	0.64	2.33	0.80
PARCS 2G	-	0.82	-	0.62	-	0.46
PARCS 4G	-	-	-	-	-	-
PARCS 8G	-	-	-	-	-	-
SKETCH-INS	2.65	0.70	2.65	0.80	2.79	1.09
heterogeneous						
BARS	0.38	0.60	1.83	0.33	0.41	0.45
DeCART	ref	ref	ref	ref	ref	ref

Table 15. Part III, pin power %EWE

	Assembly Position					
	(A,1)	(B,2)	(C,3)	(D,4)	(E,5)	(F,6)
nodal						
CORETRAN 1/FA	8.89	1.20	9.77	8.06	9.52	9.21
CORETRAN 4/FA	-	-	-	-	-	-
EPISODE	5.29	0.99	4.94	3.41	4.96	7.73
NUREC	3.49	1.07	3.23	1.09	3.35	1.87
PARCS 2G	-	1.83	-	1.39	-	0.90
PARCS 4G	-	-	-	-	-	-
PARCS 8G	-	-	-	-	-	-
SKETCH-INS	4.33	1.13	4.27	1.82	4.53	3.02
heterogeneous						
BARS	0.72	0.92	2.81	0.60	0.76	0.80
DeCART	ref	ref	ref	ref	ref	ref

Figure 8. Part III, axial power distribution

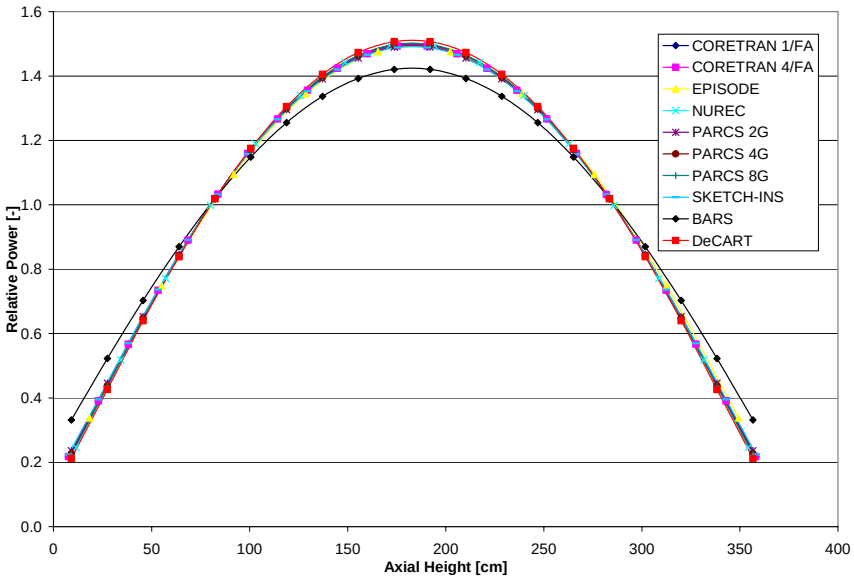

Figure 9. Part III, axial power distribution error

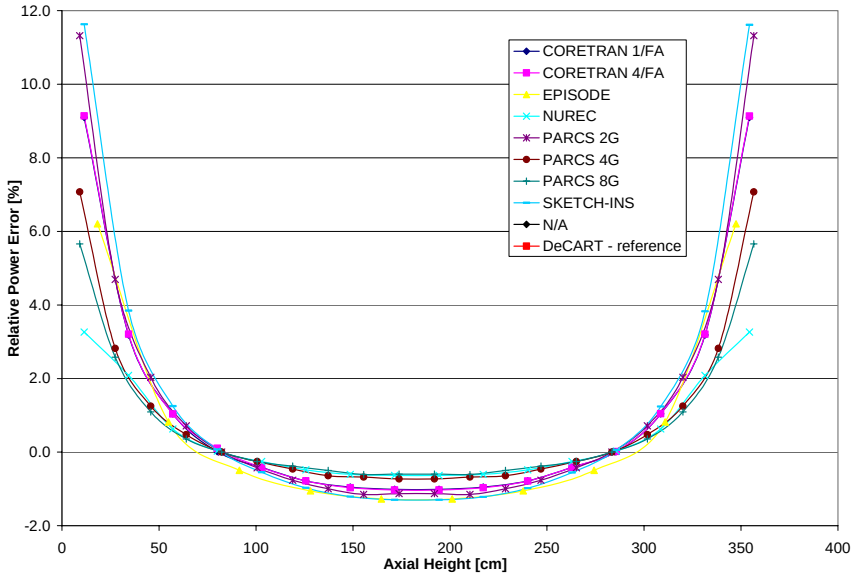

4.4 Comparison of Part IV – 3-D transient rod withdrawal from Part III conditions

Solutions were submitted for Part IV of the benchmark by all of the nodal codes and one of the heterogeneous codes, BARS. The transient results were not compared to any reference. Because of that, all of the transient results are only compared qualitatively.

A comparison of peak time, peak power, peak reactivity and power integral is shown in Table 16. All nodal results are consistent with each other but the heterogeneous BARS solution is significantly different. Excluding the BARS results, the difference between the highest and the lowest peak time, peak power, peak reactivity and power integral is only 0.04 sec, 32%, 0.06$ and 4.3%-sec, respectively.

Table 16. Part IV, comparison of peak time, peak power, peak reactivity and power integral

	Peak Time [sec]	Peak Power [%]	Peak Reactivity [$]	Power Integral [%-sec]
nodal				
CORETRAN 1/FA	0.35	140	1.08	24.8
CORETRAN 4/FA	0.33	166	1.14	26.4
EPISODE	0.33	160	1.13	26.9
NUREC	0.36	139	-	28.4
PARCS 2G	0.34	142	1.12	27.2
PARCS 4G	0.33	152	1.12	27.8
PARCS 8G	0.32	172	1.14	29.1
SKETCH-INS	0.34	144	1.12	28.0
heterogeneous				
BARS	0.21	522	1.29	41.7

It is worthwhile to note that the two effects studied in detail for the steady-state conditions, the discretisation effect in CORETRAN and the group effect in PARCS, do not significantly impact the power integral during the transient. In particular, the difference in the CORETRAN 1/FA and 4/FA

solutions is a 26% increase in transient peak power, but only 6% increase in the power integral. The difference in the PARCS 2G and 8G solutions is a 30% increase in the transient peak power, but only 7% increase in the power integral.

Transient core power is shown in Figure 10, followed by transient reactivity in Figure 11. All results, except BARS, are in a very good agreement and reflect results shown in Table 16.

Figure 10. Part IV, transient core power

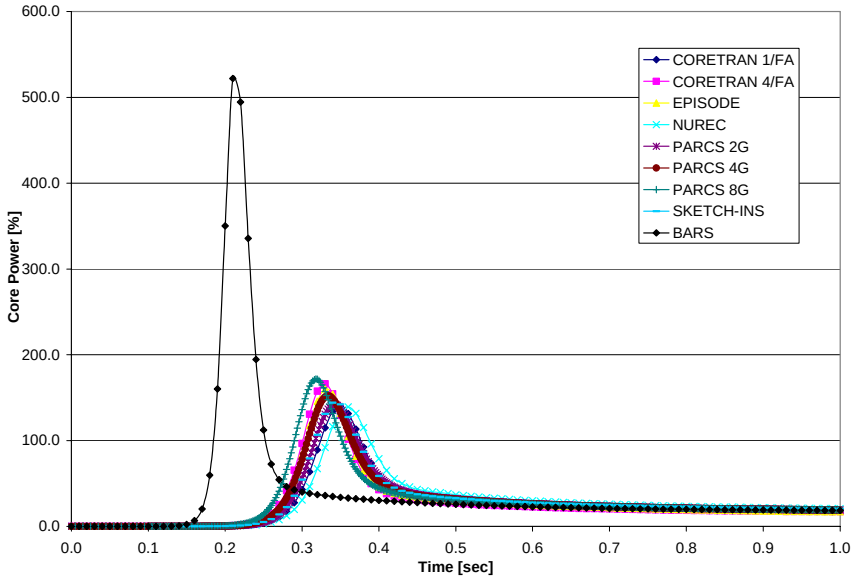

Figure 11. Part IV, transient reactivity

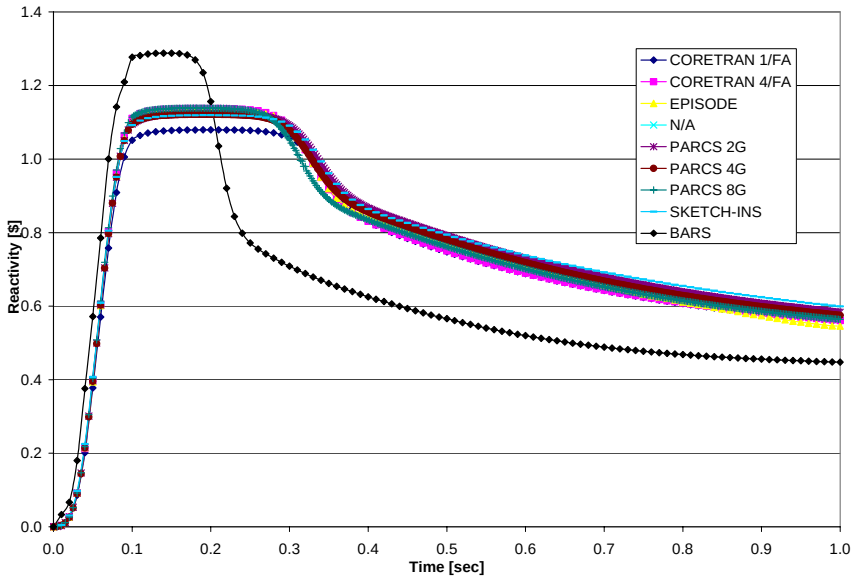

The significant difference in BARS transient results is a direct consequence of the different radial and axial power shape described in Part III of the benchmark. BARS power shape is sufficiently different to result in significantly different ejected rod worth, which results in a significantly different transient behaviour. The difference was attributed to the neutron cross-sections and unfortunately could not be resolved in a consistent manner.

Transient assembly peaking and maximum point pin peaking are shown in Figures 12 and 13, respectively. All nodal results are consistent in assembly peaking, but differ somewhat in point pin peaking. The differences in the three distinct groups of nodal solutions, one for CORETRAN, one for PARCS and SKETCH-INS and one for NUREC, are attributable to differences in pin-power reconstruction methods.

Figure 12. Part IV, transient assembly peaking

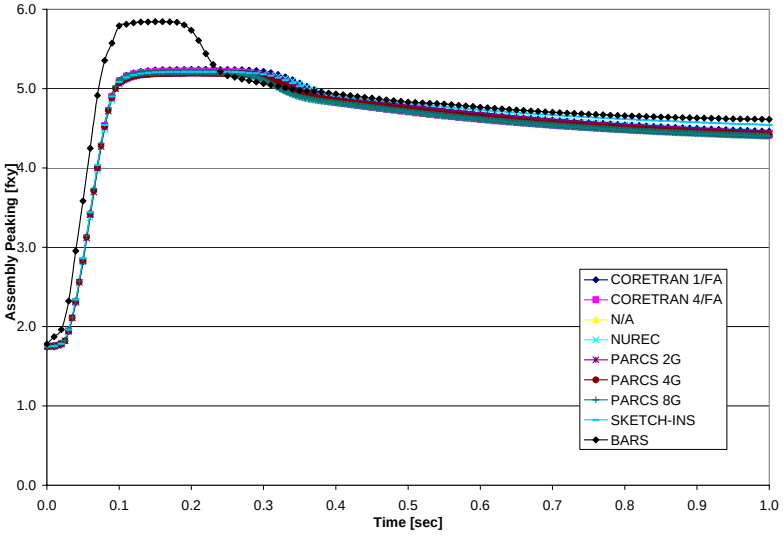

Figure 13. Part IV, transient point pin peaking

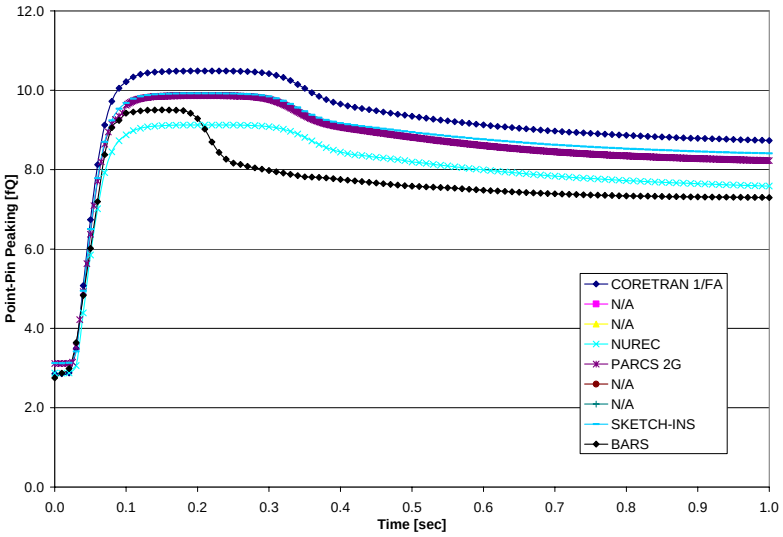

Transient core average Doppler temperature is shown in Figure 14. All results, except BARS, are in a good agreement and consistent with earlier results.

Figure 14. Part IV, transient core average Doppler temperature

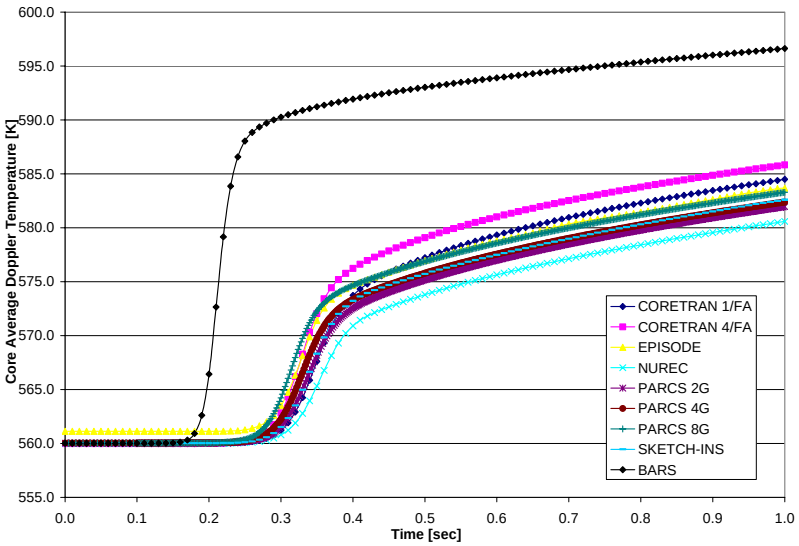

Transient core average moderator density and moderator temperature are shown in Figures 15 and 16, respectively. The two figures show the importance of using a consistent water properties table. Since CORETRAN and EPISODE appear to be using different water properties than other participants, they face the problem of matching the desired initial moderator temperature or moderator density. For this problem the neutronic feedback depends on the moderator density, not on the moderator temperature. Therefore, it is more appropriate to artificially adjust moderator temperature to obtain the desired moderator density, as was done in the EPISODE code.

Figure 15. Part IV, transient core average moderator density

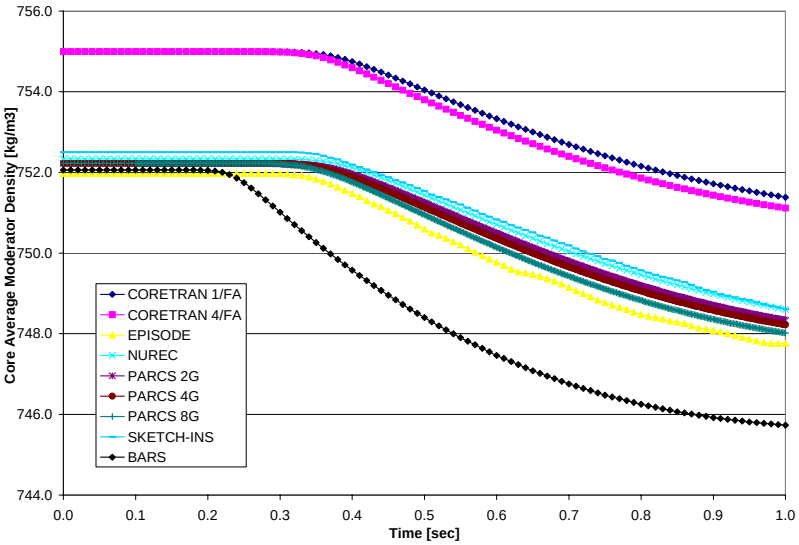

Figure 16. Part IV, transient core average moderator temperature

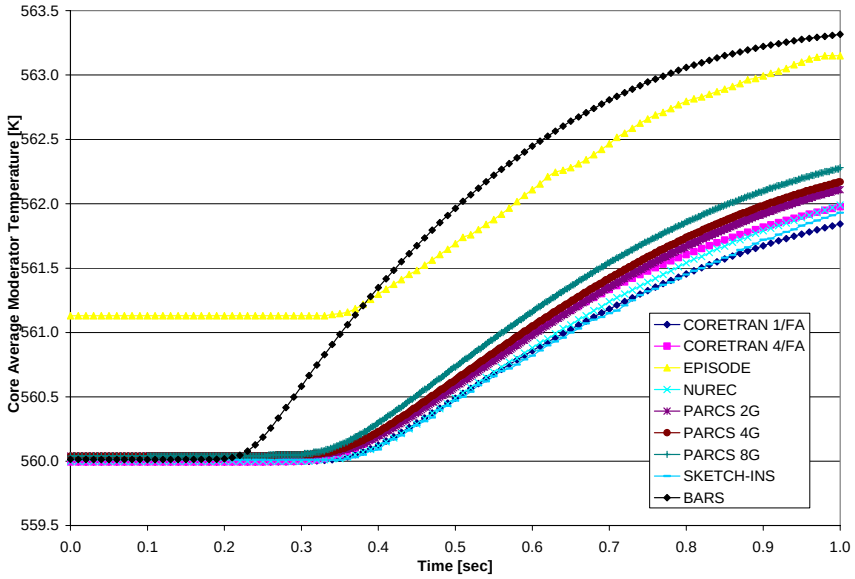

Chapter 5

CONCLUSIONS

All nodal diffusion codes were found to be capable of modelling the static MOX core, with only minor differences between results due to spatial discretisation, cross-sections interpolation and the pin-power reconstruction method. The relative difference compared to multi-group heterogeneous transport reference was found to be 1-2% relative assembly power distribution for the un-rodded state and 2-4% relative assembly power distribution for the heavily rodded state. Similar relative errors were found for static pin-power prediction.

All nodal diffusion codes were found to give consistent results for the transient solution of the MOX core, with the only differences between results due to spatial and temporal discretisation, cross-section feedback and interpolation and pin-power reconstruction method. A consistent comparison with a higher order transient method was not possible at the time of the preparation of the report because an appropriate heterogeneous solution method was not yet available.

It was found that the spatial discretisation and energy group effects are not very significant for this problem. This conclusion can probably be generalised to other LWR transients as well. The difference between used 1/FA and 4/FA discretisation method was a 26% increase in transient peak power, but only 6% increase in the power integral. The difference between 2G diffusion and 8G diffusion was a 30% increase in transient peak power, but only 7% increase in the power integral.

The submittal results summarised in Table 2 suggest that the heterogeneous transport core simulators still require some improvement, although currently the limits appear to be due to the computational resources rather than the neutronic methods. Parts of the benchmark were purposefully designed to push the limits of the capabilities of current core simulators. Because of its complexity, not all of the references were calculated with full core, multi-group heterogeneous transport method. This will allow the benchmark to be applicable to continuing code development and the capability of future full core multi-group heterogeneous transport core simulators can be assessed by this benchmark.

REFERENCES

[1] Finnemann, H., A. Galati, *NEACRP 3-D LWR Core Transient Benchmark*, NEACRP-L-335, http://www.nea.fr/html/science/docs/1991/, October 1991.

[2] Kozlowski, T., T.J. Downar, *OECD/NEA and US NRC PWR MOX/UO_2 Core Transient Benchmark, Final Specifications, Revision 2*, NEA/NSC/DOC(2003)20, December 2003, https://engineering.purdue.edu/PARCS/MOX_Benchmark.

Appendix A

BENCHMARK SPECIFICATIONS

OECD/NEA AND US NRC PWR MOX/UO_2 CORE TRANSIENT BENCHMARK

Final Specifications, Revision 2

December 2003

Tomasz Kozlowski, Thomas J. Downar
Purdue University
West Lafayette, Indiana
USA

Introduction

Computational benchmarks based on well-defined problems with a complete set of input and a unique solution are often used as a means of verifying the reliability of numerical solutions. The problems usually employ some simplifications in order to make the analysis manageable and to enable the consistent comparison of several different models, yet complex enough to make the problem applicable to actual core designs.

The present benchmark is designed to provide the framework to assess the ability of modern reactor kinetic codes to predict the transient response of a core partially loaded with MOX fuel. This benchmark employs many of the characteristics of the NEACRP L-335 PWR benchmark proposed by Finnemann in 1991 [Finnemann, 1991] which was designed to assess the ability of spatial kinetics codes to model rod ejection transients. The current problem adds the complexity of modelling a rod eject in a core fuelled partially with weapons-grade MOX. The core chosen for the simulation is based on four-loop Westinghouse PWR power plant similar to the reactor chosen for plutonium disposition in the US.

The rod ejection may occur in a PWR as a consequence of the rupture of the drive mechanism casing located on the reactor pressure vessel. This event is of particular concern for MOX-fuelled cores since the delayed neutron fraction in MOX fuel is significantly smaller than UO_2 cores. The rod ejection transient can result in significant, localised perturbations of the neutronic and thermo-hydraulic core parameters which can be difficult for reactor core simulators to predict accurately, particularly in a heterogeneous MOX-fuelled core. The problem geometry simulated here is a full PWR core in order to allow the realistic simulation of a single rod ejection.

The problem is designed primarily to assess core simulators, therefore, few-group constants are specified at the level of homogenised assembly and homogenised pin cells. However, some participants may wish to utilise their own cross-section generation codes or to model explicitly the heterogeneous pins in their core simulators. Therefore, the benchmark also specifies material compositions and pin geometries in order to reach the widest range of participants and to be applicable to continuing code developments in which heterogeneous full core transport transients are becoming possible.

This work has been performed under the auspices of OECD/NEA Working Party on the Physics of Plutonium Fuels and Innovative Fuel Cycles (WPPR). It is sponsored by the US NRC and OECD/NEA.

1) Problem statement

The objective of this problem is to evaluate core simulators through the following sequence of calculations:

a) multiplication factor, rod worth, assembly and pin power at fixed T-H conditions;

b) critical boron concentration, assembly and pin power at HFP and HZP;

c) ejection of control rod transient from HZP conditions.

HFP conditions correspond to the core power of 100.0% rated power (3 565 MW), inlet coolant temperature of 560 K, inlet pressure of 15.5 MPa. HZP conditions correspond to the core power of 10^{-4}% rated power, inlet coolant temperature of 560 K, inlet pressure of 15.5 MPa. Annex A contains submittal checklists with detailed conditions for all calculations.

The rod is assumed to be fully ejected in 0.1 seconds after which no reactor scram is considered. The control rod ejection is to be performed from HZP, all control banks in, all shutdown banks out, critical boron concentration with the highest worth rod at such condition. During the entire calculation the boron concentration and the position of the other control rods are assumed to be constant. The transient is to be calculated for 1.0 sec.

2) Core configuration (1/4 core)

Figure 1. Core configuration

	1	2	3	4	5	6	7	8
A	U 4.2% (CR-D) 35.0	U 4.2% 0.15	U 4.2% (CR-A) 22.5	U 4.5% 0.15	U 4.5% (CR-SD) 37.5	M 4.3% 17.5	U 4.5% (CR-C) 0.15	U 4.2% 32.5
B	U 4.2% 0.15	U 4.2% 17.5	U 4.5% 32.5	M 4.0% 22.5	U 4.2% 0.15	U 4.2% (CR-SB) 32.5	M 4.0% 0.15	U 4.5% 17.5
C	U 4.2% (CR-A) 22.5	U 4.5% 32.5	U 4.2% (CR-C) 22.5	U 4.2% 0.15	U 4.2% 22.5	M 4.3% 17.5	U 4.5% (CR-B) 0.15	M 4.3% 35.0
D	U 4.5% 0.15	M 4.0% 22.5	U 4.2% 0.15	M 4.0% 37.5	U 4.2% 0.15	U 4.5% (CR-SC) 20.0	M 4.3% 0.15	U 4.5% 20.0
E	U 4.5% (CR-SD) 37.5	U 4.2% 0.15	U 4.2% 22.5	U 4.2% 0.15	U 4.2% (CR-D) 37.5	U 4.5% 0.15	U 4.2% (CR-SA) 17.5	
F	M 4.3% 17.5	U 4.2% (CR-SB) 32.5	M 4.3% 17.5	U 4.5% (CR-SC) 20.0	U 4.5% 0.15	M 4.3% 0.15	U 4.5% 32.5	
G	U 4.5% (CR-C) 0.15	M 4.0% 0.15	U 4.5% (CR-B) 0.15	M 4.3% 0.15	U 4.2% (CR-SA) 17.5	U 4.5% 32.5		
H	U 4.2% 32.5	U 4.5% 17.5	M 4.3% 35.0	U 4.5% 20.0				

Assembly Type	
CR Position	
Burnup [GWd/t]	
Fresh	
Once Burn	
Twice Burn	

CR-A	Control Rod Bank A
CR-B	Control Rod Bank B
CR-C	Control Rod Bank C
CR-D	Control Rod Bank D
CR-SA	Shutdown Rod Bank A
CR-SB	Shutdown Rod Bank B
CR-SC	Shutdown Rod Bank C
CR-SD	Shutdown Rod Bank D
O	Ejected Rod

A simplified 3-D geometry was adopted for the benchmark purposes. The core has uniform fuel composition in axial direction with axial reflector of the same width as the fuel assembly pitch. Axial reflector contains fixed moderator at the same condition as the core inlet and outlet for the bottom and top axial reflector, respectively. The axial boundary condition is zero flux. Part I of the benchmark (fixed T-H conditions) is a pure 2-D problem, with no axial reflector and reflective boundary conditions in the axial direction.

The core is surrounded by a single row of reflector assemblies of the same width as the fuel assembly pitch. Each reflector assembly contains 2.52-cm thick baffle and has fixed moderator at the same condition as the core inlet. The outer radial boundary condition is zero flux.

The core was designed based on the following guidelines proposed for cores partially loaded with MOX fuel:

- no fresh MOX on the core periphery;
- no MOX assemblies facing each other;
- no MOX assemblies in control rod position;
- maximum 1/3 of the core loaded with MOX fuel;
- no integral fuel burnable absorbers (IFBA) in MOX assemblies;
- a three-batch equilibrium cycle with:
  - once-burned fuel average burn-up of 20.0 GWd/tHM;
  - twice-burned fuel average burn-up of 35.0 GWd/tHM;
- a core refuelling strategy shown in Table 1.

Table 1. Core refuelling strategy

Assembly type	Fresh fuel 0 GWd/tHM	Once-burned 20.0 GWd/tHM	Twice-burned 35.0 GWd/tHM
UO_2 4.2%	28	28	17
UO_2 4.5%	24	24	20
MOX 4.0%	8	8	4
MOX 4.3%	12	12	8
Total	72	72	49

Fuel design parameters typical of Westinghouse fuel assemblies were used in the core as shown in Table 2.

Table 2. Core design parameters

Number of fuel assemblies	193
Power level (MW_{th})	3 565
Core inlet pressure (MPa)	15.5
Hot full power (HFP) core average moderator temperature (K)	580.0
Hot zero power (HZP) core average moderator temperature (K)	560.0
Hot full power (HFP) core average fuel temperature (K)	900.0
Fuel lattice, fuel rods per assembly	17×17, 264
Number of control rod guide tubes	24
Number of instrumentation guide tubes	1
Total active core flow (kg/sec)	15 849.4
Active fuel length (cm)	365.76
Assembly pitch (cm)	21.42
Pin pitch (cm)	1.26
Baffle thickness (cm)	2.52
Design radial pin-peaking (F_H)	1.528
Design point-wise peaking (F_Q)	2.5
Core loading (tHM)	81.6
Target cycle length (GWd/tHM) (months)	21.564 (18)
Capacity factor (%)	90.0
Target effective full power days	493
Target discharge burn-up (GWd/tHM)	40.0-50.0
Maximum pin burn-up (GWd/tHM)	62.0
Shutdown margin (SDM) (%Δρ)	1.3

3) Fuel assembly configuration

The configurations for the UO_2 and MOX fuel assemblies are shown in Figures 2 and 3.

Figure 2. UO_2 fuel assembly with 104 IFBA pins

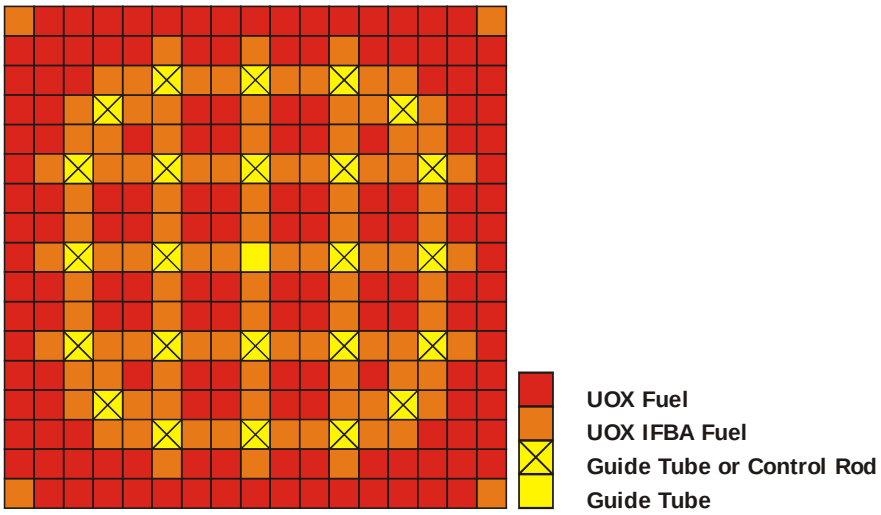

Figure 3. MOX fuel assembly with 24 WABA pins

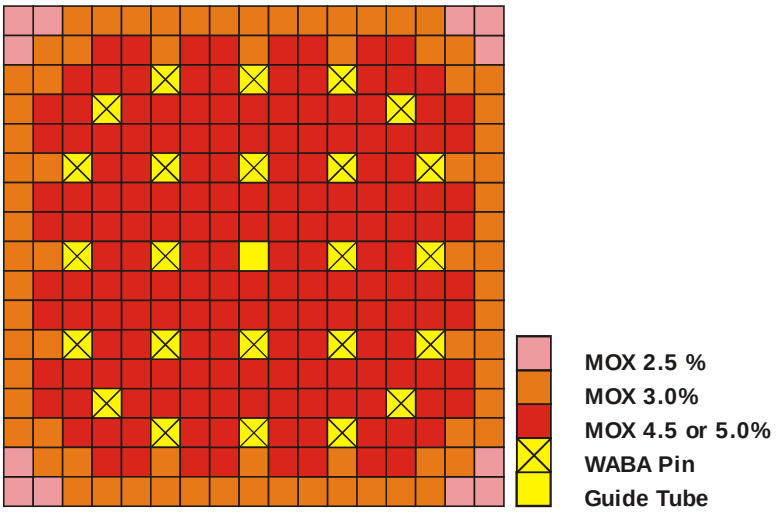

4) Material compositions

The material compositions for each of the fuel pin types are specified in Tables 3, 4 and 5.

Table 3. Heavy metal composition in fuel

Assembly type	Density [g/cm^3]	HM material	
UO_2 4.2%	10.24	^{235}U: 4.2 wt.%, ^{238}U: 95.8 wt.%	
UO_2 4.5%	10.24	^{235}U: 4.5 wt.%, ^{238}U: 95.5 wt.%	
MOX 4.0%	10.41	Corner zone: 2.5 wt.% Pu-fissile	Uranium vector: 234/235/236/238 = 0.002/0.2/0.001/99.797 wt.% Plutonium vector: 239/240/241/242 = 93.6/5.9/0.4/0.1 wt.%
		Peripheral zone: 3.0 wt.% Pu-fissile	
		Central zone: 4.5 wt.% Pu-fissile	
MOX 4.3%	10.41	Corner zone: 2.5 wt.% Pu-fissile	
		Peripheral zone: 3.0 wt.% Pu-fissile	
		Central zone: 5.0 wt.% Pu-fissile	

Table 4. Other burnable materials

Absorber material	Density [g/cm^3]	Material
Control rod	1.84	B_4C
IFBA	1.69	ZrB_2
WABA	3.5635	Al_2O_3-B_4C, 10.0 wt.% B_4C

Table 5. Other non-burnable materials

Other material	Density [g/cm^3]	Material
Clad	6.504	Zircaloy-2: Zr/Sn/Fe/Cr/N = 98.23/1.50/0.12/0.10/0.05 at.%
Gap	0.001	^{16}O
Baffle	7.82	SS-304: Fe/Cr/Ni/Mn = 70.351/19.152/8.483/2.014 at.%
Coolant	0.75206	Water at 560 K and 15.5 MPa
Coolant	0.71187	Water at 580 K and 15.5 MPa
Coolant	0.66114	Water at 600 K and 15.5 MPa

All boron contains B-10/B-11 = 19.9/80.1 at.%. The same type of Zircaloy-2 material is used as cladding for fuel pin, guide tube, control rod and WABA.

Integral fuel burnable absorber (IFBA) pins are used for the reactivity control of the UO_2 assemblies. IFBA is a coating of zirconium diboride (ZrB_2) on the fuel pellets and provides reactivity control over a relatively short burn-up period. All UO_2 assemblies are designed to contain 104 IFBA pins and are located in the highest worth regions in the vicinity of the guide tubes and corners of the assembly.

Wet annular burnable absorber (WABA) pins are used for reactivity control of the MOX assemblies. WABA consists of an annular pellet of Al_2O_3-B_4C with wet (water-filled) central region and Zircaloy cladding. In contrast to IFBA, WABA provides relatively long-term reactivity control. All MOX assemblies are designed with 24 WABA pins inserted in the guide tube locations.

Even though all necessary macroscopic cross-sections are provided as a part of the benchmark specifications, the material number densities are also specified. This was done in order to attract future participants when full-core heterogeneous modelling (fuel/clad/moderator) becomes more common. In addition, it allows participants to use their own cross-section generation methodology or if a participant is unable to use macroscopic cross-sections provided in the benchmark.

Fuel, WABA and IFBA number densities are provided at each burn-up point. Since HELIOS tracks 142 isotopes for the fuel, the data set becomes very large. The data is reduced by including only isotopes with number density greater than 10^{-9} atoms/barn-cm. It is assumed that all fuel pins of the same type within the assembly have the same burn-up. The data file is available in electronic form on the benchmark website and by request from the benchmark organisers. A sample with the first 65 isotopes for UO_2 4.2% fuel is shown in Annex B.

5) Pin cell geometry specifications

The dimensions of the pin cells are listed in Tables 6 and 7, and shown in Figure 4. The Cr-clad and WABA-clad gap is ignored and replaced with clad.

Table 6. Pin cell dimensions [cm]

Cell type/ radius	Fuel	IFBA	GT	CR	WABA
r1	0.3951	0.3951	0.5624	0.4331	0.2858
r2	0.4010	0.3991	0.6032	0.4839	0.3531
r3	0.4583	0.4010		0.5624	0.4039
r4		0.4583		0.6032	0.4839
r5					0.5624
r6					0.6032

Table 7. Pin cell materials

Cell type/ radius	Fuel	IFBA	GT	CR	WABA
r0-r1	Fuel	Fuel	Water	Cr	Water
r1-r2	Gap	IFBA	Clad	Clad	Clad
r2-r3	Clad	Gap		Water	WABA
r3-r4		Clad		Clad	Clad
r4-r5					Water
r5-r6					Clad

Figure 4. Pin cell geometry

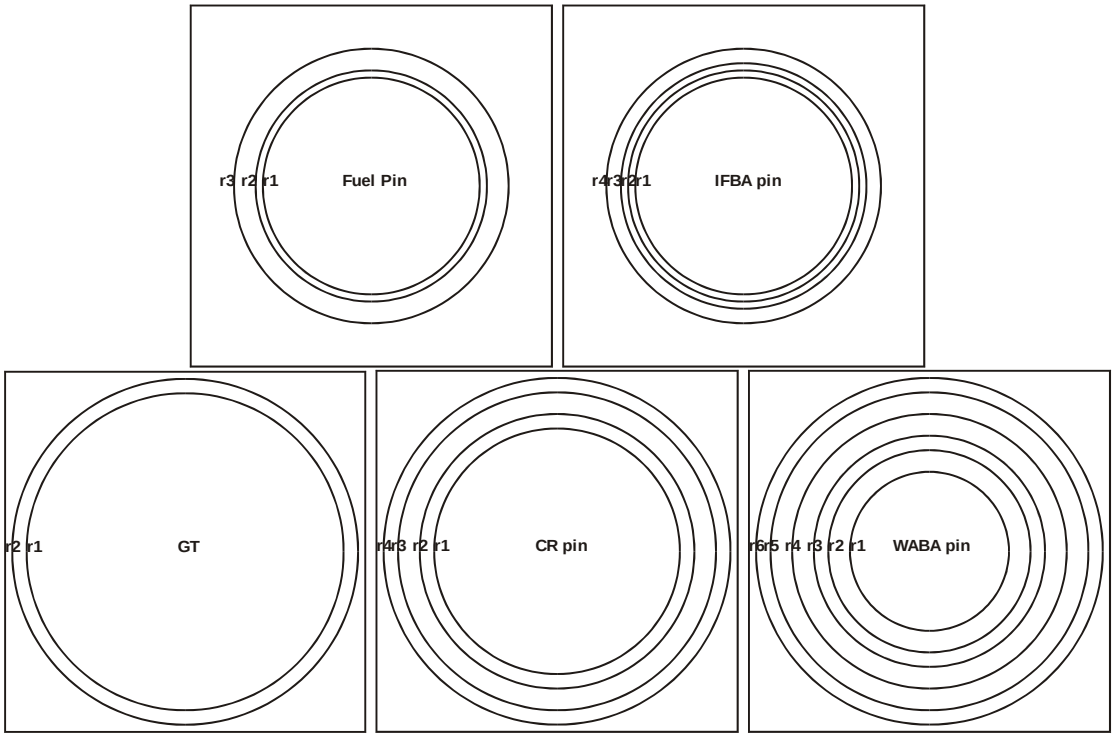

6) Cross-section modelling information

The benchmark is intended as an assembly heterogeneous benchmark (cell homogeneous or cell heterogeneous, i.e. fuel/clad/moderator). However, it is assumed that not all participants have the same capabilities in their core simulators and that some participants might want to use different levels of homogenisation detail. Therefore, the following XS homogenisation levels and group structures are made available in the benchmark specifications:

- 2G assembly homogenised XS with discontinuity factors and pin power form functions;
- 4G assembly homogenised XS with discontinuity factors and pin power form functions;
- 8G pin-cell homogenised XS.

A complete set of macroscopic cross-sections and kinetic parameters defined for each assembly or cell type are provided in the NEMTAB-like format used for the OECD MSLB benchmark [Ivanov, 1999]. The format is described in Annex C. The cross-sections were calculated at different fuel temperature, moderator density and boron density conditions to cover the expected range of core operating conditions. The branch conditions at which cross-sections were calculated are shown on Figure 5. The moderator temperature effect is treated implicitly in the moderator density term assuming constant pressure of 15.5 MPa. It is expected that participants using full-core heterogeneous models will use the cross-section libraries native to their own codes and the difference will be accounted for during the analysis of results.

Figure 5. Cross-section branch model

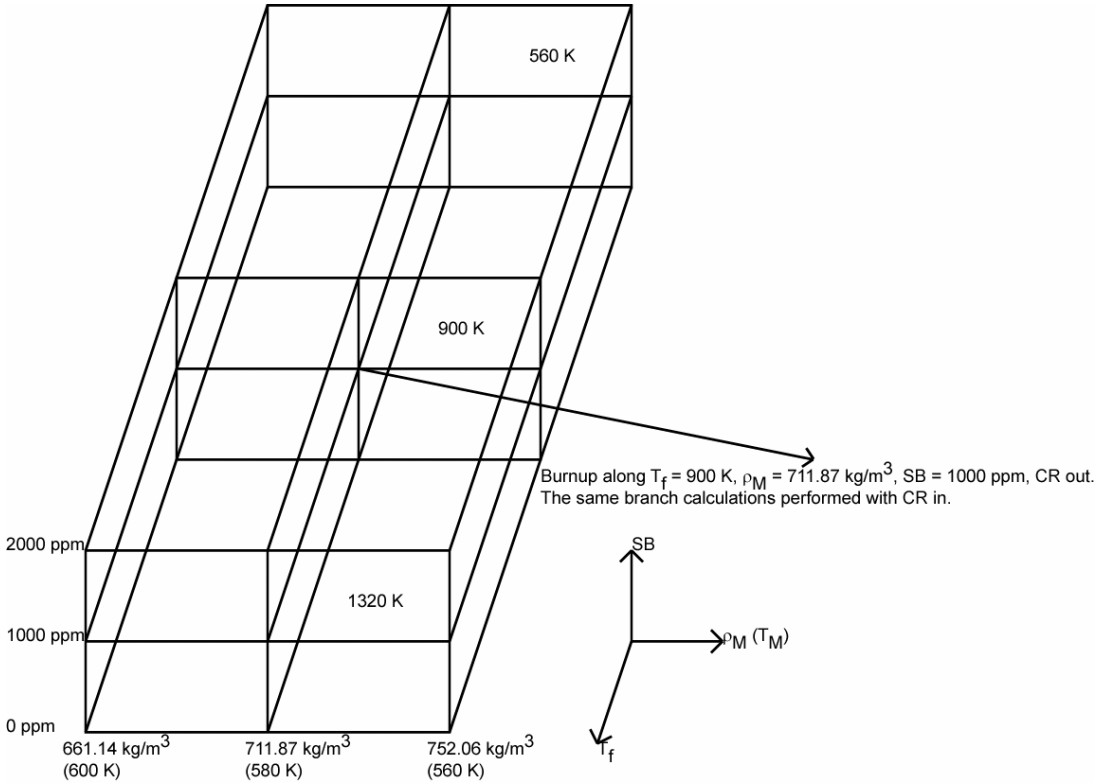

The energy group structure for the cell and assembly homogenised cross-sections are shown in Table 8. The two-group structure uses the standard 0.625 eV energy cut-off. The upscattering in the two- and four-group cross-sections was removed by modifying the downscattering using the conservation of neutron spectra to treat the up-scattering effect implicitly:

$$\Sigma_{g' \leftarrow g} = \Sigma_{g' \leftarrow g} - \frac{\phi_{g'}}{\phi_g} \Sigma_{g \leftarrow g'}, \; g < g' \tag{1}$$

Table 8. Energy group structure

4-group structure	8-group structure	Lower energy cut-off [eV]
1	1	2.2313E+06
	2	8.2085E+05
	3	9.1188E+03
2	4	1.3007E+02
	5	3.9279E+00
3	6	6.2506E-01
4	7	1.4572E-01
	8	0.0000E+00

7) Thermal-physical properties

The effective Doppler temperature T_f is to be determined from the fuel rod centreline temperature $T_{f,C}$ and the fuel rod surface temperature $T_{f,S}$:

$$T_f = (1-\alpha) T_{f,C} + \alpha T_{f,S} \tag{2}$$

where α is taken to equal 0.7. This relation is assumed to apply for both UO_2 and MOX fuel.

The following simplified fuel thermal-physical properties are provided [Finnemann, 1991]:

$$k_{UO2} = 1.05 + \frac{2150}{T - 73.15} \; \frac{W}{m \cdot K} \tag{3}$$

$$k_{Zr-2} = 7.51 + 2.09 \cdot 10^{-2} T - 1.45 \cdot 10^{-5} T^2 + 7.67 \cdot 10^{-9} T^3 \; \frac{W}{m \cdot K} \tag{4}$$

$$c_{p,UO2} = 162.3 + 0.3038T - 2.391 \cdot 10^{-4} T^2 + 6.404 \cdot 10^{-8} T^3 \; \frac{J}{kg \cdot K} \tag{5}$$

$$c_{p,Zr-2} = 252.54 + 0.11474T \; \frac{J}{kg \cdot K} \tag{6}$$

Since MOX fuel thermal conductivity is about 10% smaller than the UO_2 fuel, for the purposes of the benchmark the MOX fuel thermal conductivity is calculated as:

$$k_{MOX} = 0.9 k_{UO2} \tag{7}$$

The heat transfer coefficient for the gap between fuel and cladding is assumed to be constant:

$$h_{gap} = 10^4 \ \frac{W}{m^2 \cdot K} \tag{8}$$

Expansion effects of fuel and cladding are not considered in this benchmark and are treated implicitly by providing fuel dimensions and densities at HFP conditions. The heat transfer coefficient between cladding and moderator should be calculated using code specific correlations. Because this is a very fast transient from hot zero power conditions, any variation in the manner of calculating these parameters should not be important for this benchmark. It is expected that the T-H feedback would be performed in a manner consistent with the neutronics model (e.g. pin-wise or assembly-wise) and any differences among participants will be accounted for in the analysis of results.

8) Benchmark submittal

The submittal should be made on the Excel submittal templates that are part of the benchmark. If Excel is not available, another format will be provided by request. The submittal should be sent to both tomasz@ecn.purdue.edu and downar@ecn.purdue.edu by 1 June 2004. No paper copy is necessary.

A benchmark website has been established at:

https://engineering.purdue.edu/PARCS/MOX_Benchmark

The website will make available the specifications, material number densities, cross-section libraries, Excel submittal templates, answers to questions and any updates made since release of the benchmark.

Organisers contact information:

Tomasz Kozlowski
Purdue University
1290 Nuclear Engineering Building
West Lafayette, IN 47907
USA
tomasz@ecn.purdue.edu
Tel. +1-765-494-7828
Fax. +1-765-494-9570

Prof. Thomas J. Downar
Purdue University
1290 Nuclear Engineering Building
West Lafayette, IN 47907
USA
downar@ecn.purdue.edu
Tel. +1-765-494-5752
Fax. +1-765-494-9570

Please notify benchmark organisers via email your intent to participate in the benchmark.

REFERENCES

[1] Alsaed, A.A., M.L. Adams, *Disposition of Weapons-grade Plutonium in Westinghouse Reactors*, ANRCP-1998-1, http://www.pu.org/, March 1998.

[2] Alonso-Vargas, G., M.L. Adams, *Studies of Flexible MOX/LEU Fuel Cycles*, ORNL/SUB/99-19XSY062V-1, ANRCP-1999-9, http://www.pu.org/, March 1999.

[3] Cho, N.Z., *Benchmark Problem 1A*, KAIST/NurapT, http://nurapt.kaist.ac.kr/benchmark/, June 2000.

[4] Finnemann, H., A. Galati, *NEACRP 3-D LWR Core Transient Benchmark*, NEACRP-L-335, http://www.nea.fr/html/science/docs/1991/, October 1991.

[5] Lefebvre, J.C., J. Mondot, J.P. West, *Benchmark Calculations of Power Distribution Within Assemblies*, NEACRP L-336, http://www.nea.fr/html/science/docs/1991/, October 1991.

[6] Ivanov, K.N., T.M. Beam, A.J. Baratta, *PWR Main Steam Line Break (MSLB) Benchmark, Volume I: Final Specifications*, NEA/NSC/DOC(99)8, http://www.nea.fr/html/science/docs/1999/, April 1999.

Annex A

SUBMITTAL CHECKLIST

Part I: 2-D fixed T-H conditions (ρ_M = 752.06 kg/m^3, T_{core} = 560 K, SB = 1000.0 ppm)

a) All rods out state
___ k_{eff}
___ axially averaged assembly power
___ axially averaged pin power for 6 assemblies along the diagonal (A,1) - (F,6)

b) Rod worth calculations with all rods out
___ k_{eff} with Rod (A, 1) in
___ k_{eff} with Rod (A, 3) in
___ k_{eff} with Rod (A, 5) in
___ k_{eff} with Rod (A, 7) in
___ k_{eff} with Rod (B, 6) in
___ k_{eff} with Rod (C, 3) in
___ k_{eff} with Rod (C, 7) in
___ k_{eff} with Rod (D, 6) in
___ k_{eff} with Rod (E, 5) in
___ k_{eff} with Rod (E, 7) in

c) All rods in state
___ k_{eff}
___ axially averaged assembly power
___ axially averaged pin power for 6 assemblies along the diagonal (A,1) - (F,6)

d) Rod worth calculations with all rods in
___ k_{eff} with Rod (A, 1) out
___ k_{eff} with Rod (A, 3) out
___ k_{eff} with Rod (A, 5) out
___ k_{eff} with Rod (A, 7) out
___ k_{eff} with Rod (B, 6) out
___ k_{eff} with Rod (C, 3) out
___ k_{eff} with Rod (C, 7) out
___ k_{eff} with Rod (D, 6) out
___ k_{eff} with Rod (E, 5) out
___ k_{eff} with Rod (E, 7) out

Part II: 3-D HFP conditions (power = 100.0%, T_{in} = 560 K, P_{in} = 15.5 MPa, SB = critical)

a) All rods out state
___ critical boron concentration
___ axially averaged assembly power
___ axially averaged pin power for 6 assemblies along the diagonal (A,1) - (F,6)
___ axially averaged assembly Doppler temperature
___ axially averaged assembly moderator density
___ axially averaged assembly moderator temperature
___ assembly moderator density at core outlet
___ assembly moderator temperature at core outlet
___ radially averaged axial power
___ radially averaged axial Doppler temperature
___ radially averaged axial moderator density
___ radially averaged axial moderator temperature

Part III: 3-D HZP conditions (power = 10^{-4}%, T_{in} = 560 K, P_{in} = 15.5 MPa, SB = critical)

a) Beginning of transient: all control banks in, all shutdown banks out state
___ critical boron concentration
___ core β_{eff}
___ axially averaged assembly power
___ axially averaged pin power for 6 assemblies along the diagonal (A,1) - (F,6)
___ radially averaged axial power

Part IV: 3-D transient: withdrawal of rod (E, 5) from conditions calculated in Part III.a

a) Provide every 0.01 sec up to 1.0 sec
___ core power
___ total reactivity
___ Doppler reactivity
___ moderator reactivity
___ control rod reactivity
___ radial assembly peaking (f_{xy})
___ radial pin peaking (f_H)
___ point-wise pin peaking (f_Q)
___ core average Doppler temperature
___ core average moderator density
___ core average moderator temperature

b) Provide every 0.1 sec up to 1.0 sec
___ axially averaged assembly power
___ axially averaged pin power for 6 assemblies along the diagonal (A,1) - (F,6)
___ assembly axial power in the location of the ejected rod
___ assembly axial Doppler temperature in the location of the ejected rod
___ assembly axial moderator density in the location of the ejected rod
___ assembly axial moderator temperature in the location of the ejected rod

Annex B

SAMPLE FUEL NUMBER DENSITIES FOR UO_2 4.2% ASSEMBLY

		Burnup [GWd/t]							
		Burnup Point							
Isotope	**HELIOS**	**0.0**	**0.15**	**17.5**	**20.0**	**22.5**	**32.5**	**35.0**	**37.5**
Name	**Identifier**	**1**	**2**	**17**	**18**	**19**	**23**	**24**	**25**
Mo-95 (FP)	42595	-	-	1.76830E-05	2.10532E-05	2.43736E-05	3.70448E-05	4.00530E-05	4.29970E-05
Tc-99 (FP)	43599	-	8.19239E-08	2.40933E-05	2.73519E-05	3.05554E-05	4.27999E-05	4.57139E-05	4.85671E-05
Pd-108 (FP)	46608	-	3.58133E-09	2.01585E-06	2.51039E-06	3.04915E-06	5.62129E-06	6.36298E-06	7.14199E-06
Xe-131 (FP)	54631	-	1.63840E-08	1.06985E-05	1.20328E-05	1.33047E-05	1.77608E-05	1.87169E-05	1.96103E-05
Cs-133 (FP)	55633	-	5.42128E-08	2.61076E-05	2.96475E-05	3.31193E-05	4.62932E-05	4.94008E-05	5.24312E-05
U-235	92235	9.71492E-04	9.67328E-04	5.80775E-04	5.36589E-04	4.94761E-04	3.49384E-04	3.18203E-04	2.88980E-04
U-236	92236	-	7.92924E-07	7.11583E-05	7.86753E-05	8.56486E-05	1.08470E-04	1.12982E-04	1.17044E-04
U-238	92238	2.18794E-02	2.18773E-02	2.16336E-02	2.15964E-02	2.15585E-02	2.13988E-02	2.13569E-02	2.13140E-02
Pu-238	94238	-	-	5.08451E-07	7.13536E-07	9.62084E-07	2.42733E-06	2.91468E-06	3.44917E-06
Pu-239	94239	-	7.54884E-07	1.07858E-04	1.14067E-04	1.19049E-04	1.30075E-04	1.31236E-04	1.31952E-04
Pu-240	94240	-	1.43304E-09	2.21196E-05	2.60945E-05	3.00003E-05	4.43591E-05	4.75380E-05	5.05287E-05
Pu-241	94241	-	-	1.09779E-05	1.37246E-05	1.64876E-05	2.67336E-05	2.89421E-05	3.09761E-05
Pu-242	94242	-	-	1.26448E-06	1.86575E-06	2.60137E-06	6.85451E-06	8.22176E-06	9.69682E-06
Am-241	95241	-	-	1.76423E-07	2.49678E-07	3.33089E-07	7.19747E-07	8.17423E-07	9.11165E-07
O-16 in UO2	8001	4.57018E-02	4.57018E-02	4.57018E-02	4.57018E-02	4.57018E-02	4.57018E-02	4.57018E-02	4.57018E-02
Ru-101 (FP)	44601	-	1.88143E-07	2.19801E-05	2.51017E-05	2.82139E-05	4.05465E-05	4.35951E-05	4.66278E-05
Rh-103 (FP)	45603	-	4.02572E-09	1.19458E-05	1.37890E-05	1.55849E-05	2.22112E-05	2.37128E-05	2.51478E-05
Rh-105 (FP)	45605	-	1.75909E-08	4.57383E-08	4.84212E-08	5.09780E-08	6.02870E-08	6.24351E-08	6.45223E-08
Pd-105 (FP)	46605	-	2.02417E-08	7.71152E-06	9.18176E-06	1.07211E-05	1.74893E-05	1.93171E-05	2.11929E-05
Pd-107 (FP)	46607	-	8.43945E-09	3.32193E-06	4.08714E-06	4.91198E-06	8.76228E-06	9.85276E-06	1.09907E-05
Ag-109 (FP)	47609	-	2.12441E-09	1.21185E-06	1.49268E-06	1.79259E-06	3.14995E-06	3.52120E-06	3.90237E-06
In-115 (FP)	49615	-	-	9.92244E-08	1.11432E-07	1.23041E-07	1.63316E-07	1.71839E-07	1.79758E-07
Xe-134 (FP)	54634	-	2.82190E-07	3.25852E-05	3.71928E-05	4.17910E-05	6.00974E-05	6.46538E-05	6.92024E-05
Nd-143 (FP)	60643	-	9.00163E-09	1.97780E-05	2.21845E-05	2.44529E-05	3.21512E-05	3.37326E-05	3.51775E-05
Nd-145 (FP)	60645	-	1.40715E-07	1.48964E-05	1.68123E-05	1.86793E-05	2.56639E-05	2.72896E-05	2.88670E-05
Pm-147 (FP)	61647	-	9.51027E-09	5.80911E-06	6.27491E-06	6.67053E-06	7.69046E-06	7.83361E-06	7.94163E-06
Pm-148m (FP)	61748	-	-	4.84864E-08	5.24076E-08	5.56855E-08	6.35934E-08	6.45369E-08	6.51599E-08
Sm-147 (FP)	62647	-	-	1.00999E-06	1.25728E-06	1.51371E-06	2.55676E-06	2.80709E-06	3.04864E-06
Sm-149 (FP)	62649	-	1.46942E-08	1.07522E-07	1.08046E-07	1.08134E-07	1.05255E-07	1.03964E-07	1.02526E-07
Sm-150 (FP)	62650	-	2.73051E-09	5.08532E-06	5.89284E-06	6.70640E-06	9.97015E-06	1.07769E-05	1.15757E-05
Sm-151 (FP)	62651	-	9.61655E-09	4.32940E-07	4.51705E-07	4.69311E-07	5.30339E-07	5.43485E-07	5.55867E-07
Sm-152 (FP)	62652	-	1.03882E-08	2.39241E-06	2.71748E-06	3.02869E-06	4.14660E-06	4.39754E-06	4.63829E-06
Eu-153 (FP)	63653	-	2.96560E-09	1.51938E-06	1.85186E-06	2.20324E-06	3.73578E-06	4.13668E-06	4.53971E-06
Eu-154 (FP)	63654	-	-	2.17340E-07	2.85195E-07	3.61079E-07	7.25940E-07	8.27219E-07	9.30400E-07
Eu-155 (FP)	63655	-	1.32483E-09	4.96168E-08	6.03234E-08	7.23063E-08	1.31119E-07	1.47925E-07	1.65291E-07
Gd-155 (FP)	64655	-	-	-	-	-	1.20544E-09	1.35055E-09	1.49818E-09
Gd-156 (FP)	64656	-	-	4.79685E-07	6.23822E-07	7.95778E-07	1.83527E-06	2.20096E-06	2.61565E-06
Gd-157 (FP)	64657	-	-	2.01182E-09	2.21770E-09	2.43171E-09	3.40132E-09	3.67750E-09	3.96851E-09
Gd-158 (FP)	64658	-	-	1.58331E-07	1.96743E-07	2.39588E-07	4.62939E-07	5.34135E-07	6.12592E-07
U-234	92234	-	-	-	-	-	-	-	-
U-237	92237	-	8.46214E-09	1.43301E-07	1.56299E-07	1.68754E-07	2.14061E-07	2.24390E-07	2.34336E-07
Np-237	93237	-	1.85389E-09	3.69536E-06	4.49683E-06	5.33400E-06	8.88982E-06	9.79707E-06	1.06995E-05
Np-238	93238	-	-	9.14987E-09	1.13638E-08	1.37685E-08	2.51144E-08	2.83325E-08	3.16794E-08
Np-239	93239	-	1.06838E-06	1.62883E-06	1.65984E-06	1.69260E-06	1.83717E-06	1.87603E-06	1.91571E-06
Am-242m	95342	-	-	2.66668E-09	3.97286E-09	5.51556E-09	1.30393E-08	1.49824E-08	1.68500E-08
Am-243	95243	-	-	1.08442E-07	1.85480E-07	2.94289E-07	1.14358E-06	1.47677E-06	1.86212E-06
Cm-242	96242	-	-	2.60826E-08	4.18494E-08	6.23897E-08	1.91794E-07	2.34309E-07	2.79774E-07
Cm-243	96243	-	-	-	-	-	3.13637E-09	4.14652E-09	5.32356E-09
Cm-244	96244	-	-	1.20043E-08	2.40266E-08	4.39017E-08	2.70011E-07	3.83945E-07	5.30227E-07
Cm-245	96245	-	-	-	-	1.35307E-09	1.16135E-08	1.75815E-08	2.56871E-08
Cm-246	96246	-	-	-	-	-	-	1.19368E-09	1.94276E-09
Br-81 (FP)	35581	-	7.19542E-09	8.03959E-07	9.12825E-07	1.02009E-06	1.43280E-06	1.53182E-06	1.62918E-06
Kr-82 (FP)	36582	-	-	8.44430E-09	1.09770E-08	1.38494E-08	2.88013E-08	3.34192E-08	3.83934E-08
Kr-83 (FP)	36583	-	1.91147E-08	1.85164E-06	2.06244E-06	2.26079E-06	2.93190E-06	3.06961E-06	3.19551E-06
Kr-84 (FP)	36584	-	3.58234E-08	3.93700E-06	4.47587E-06	5.01116E-06	7.12403E-06	7.64665E-06	8.16751E-06
Kr-85 (FP)	36585	-	9.91486E-09	9.86750E-07	1.10570E-06	1.22003E-06	1.63430E-06	1.72780E-06	1.81750E-06
Kr-86 (FP)	36586	-	6.93053E-08	7.13350E-06	8.03551E-06	8.91357E-06	1.22023E-05	1.29717E-05	1.37211E-05
Sr-89 (FP)	38589	-	1.61277E-07	2.41539E-06	2.34747E-06	2.28103E-06	2.03479E-06	1.97747E-06	1.92157E-06
Sr-90 (FP)	38590	-	2.02118E-07	2.03192E-05	2.28109E-05	2.52173E-05	3.40448E-05	3.60634E-05	3.80106E-05
Y-89 (FP)	39589	-	4.51067E-09	1.45298E-05	1.67222E-05	1.88521E-05	2.67821E-05	2.86255E-05	3.04162E-05
Y-91 (FP)	39591	-	2.00633E-07	3.55081E-06	3.46700E-06	3.38252E-06	3.06275E-06	2.98793E-06	2.91497E-06
Zr-91 (FP)	40591	-	4.84189E-09	1.77237E-05	2.05119E-05	2.32316E-05	3.34443E-05	3.58388E-05	3.81729E-05
Zr-93 (FP)	40593	-	2.24830E-07	2.39695E-05	2.71046E-05	3.01778E-05	4.18822E-05	4.46669E-05	4.73970E-05
Zr-95 (FP)	40595	-	2.25745E-07	4.80109E-06	4.75775E-06	4.70800E-06	4.50053E-06	4.45032E-06	4.40110E-06
Zr-96 (FP)	40596	-	2.27071E-07	2.51684E-05	2.85976E-05	3.19918E-05	4.52378E-05	4.84704E-05	5.16727E-05
Nb-95 (FP)	41595	-	4.84915E-09	2.62471E-06	2.61063E-06	2.58774E-06	2.47646E-06	2.44870E-06	2.42142E-06

Annex C

SAMPLE 2G XS FORMAT

```
*   Mod Dens   Boron ppm   Fuel Temp    Mod Temp
       3       3       3       0
     661.14     711.87     752.06
      0.00    1000.00    2000.00
     560.00     900.00    1320.00
*
* ---------------------------------------------------------
* BURNUP  0.15
* ---------------------------------------------------------
*
* Transport XSEC Table
*
* GROUP    1
  XS(D1,B1,F1)  XS(D2,B1,F1)  XS(D3,B1,F1)
  XS(D1,B2,F1)  XS(D2,B2,F1)  XS(D3,B2,F1)
  XS(D1,B3,F1)  XS(D2,B3,F1)  XS(D3,B3,F1)
  XS(D1,B1,F2)  XS(D2,B1,F2)  XS(D3,B1,F2)
  XS(D1,B2,F2)  XS(D2,B2,F2)  XS(D3,B2,F2)
  XS(D1,B3,F2)  XS(D2,B3,F2)  XS(D3,B3,F2)
  XS(D1,B1,F3)  XS(D2,B1,F3)  XS(D3,B1,F3)
  XS(D1,B2,F3)  XS(D2,B2,F3)  XS(D3,B2,F3)
  XS(D1,B3,F3)  XS(D2,B3,F3)  XS(D3,B3,F3)
* GROUP    2
  ...
*
* Absorption XSEC Table
  ...
*
* Nu-Fission XSEC Table
  ...
*
* Kappa-Fission XSEC Table
  ...
*
* Scattering XSEC Table
*
* GROUP    1 ->      2
  ...
* GROUP    2 ->      1
  ...
*
* ADF Table
  ...
*
* Fission Spectrum
*
* GROUP    1       2
    CHI(G1)    CHI(G2)
*
* Inverse Velocity
*
* GROUP    1       2
    IVEL(G1)    IVEL(G2)
*
* Delay Neutron Decay Constant (Lambda)
*
* GROUP    1       2       3       4       5       6
```

```
   LAMBDA(G1)    LAMBDA(G2)    LAMBDA(G3)    LAMBDA(G4)    LAMBDA(G5)    LAMBDA(G6)
*
* Delay Neutron Fraction (Beta)
*
* GROUP    1        2        3        4        5        6
    BETA(G1)     BETA(G2)     BETA(G3)     BETA(G4)     BETA(G5)     BETA(G6)
*
* ------------------------------------------------------------
* BURNUP 17.50
* ------------------------------------------------------------
...
```

Annex D

DETAILS TO BE PROVIDED ABOUT THE CALCULATION SCHEME

1. Name and address of participant(s).

2. Establishment(s).

3. Name of code system(s) and computational method, angular and spatial approximation used.

4. Bibliographical references for the code.

5. Cross-section library used. If own library was used, please describe homogenisation method, number of groups and data reduction method.

6. Other assumptions and comments useful for interpreting correctly the results. Provide short description of the T-H solution.

Appendix B

CALCULATION DETAILS PROVIDED BY THE PARTICIPANTS

1. **Name and address of participant(s).**

   Hakim Ferroukhi, Hakim.Ferroukhi@psi.ch
   Martin Zimmermann, Martin.Zimmermann@psi.ch

2. **Establishment(s).**

   Laboratory for Reactor Physics and Systems Behaviour
   Paul Scherrer Institut, Villigen 5232-PSI, Switzerland

3. **Name of code system(s) and computational method, angular and spatial approximation used.**

   - CORETRAN-01 MOD001:
     - ARROTTA neutronic module (2-G nodal, ANM with quadratic leakage approximation);
     - VIPRE-02 T-H module (two-fluid, six equations).
   - Neutronic discretisation:
     - 1×1 solution: 1 node/FA;
     - 2×2 solution: 4 nodes/FA;
     - axial discretisation: 24 equidistant planes in the active fuel region, 1 plane for the top reflector, 1 plane of the bottom reflector;
     - time discretisation: Crank-Nicolson with 1 ms time step.
   - Thermal-hydraulic discretisation:
     - 193 separate flow channels with no cross-flow (full core model);
     - each T-H channel discretised in equidistant 24 axial nodes plus one at top and one at bottom.

4. **Bibliographical references for the code.**

   Eisenhart, L.D., *et al*., *CORETRAN-01: A Three-dimensional Program for Reactor Physics and Thermal-hydraulic Analysis*, EPRI Report WO-3574, Rev. 3, November 2000.

5. **Cross-section library used.**

   2G nodal library.

6. **Other assumptions and comments useful for interpreting correctly the results. Provide short description of the T-H solution.**

   Axial quantities are node average.

1. **Name and address of participant(s).**

Toshikazu Takeda, takeda@nucl.eng.osaka-u.ac.jp
Sho Tanaka, s-tanaka@stu.nucl.eng.osaka-u.ac.jp

2. **Establishment(s).**

Osaka University, Department of Nuclear Engineering, Japan

3. **Name of code system(s) and computational method, angular and spatial approximation used.**

- *Code name*: EPISODE version 1.00, multi-group nodal method (NEM).
- *Spatial discretisation*: 16 nodes/assembly radially, 20 planes for active core region and 1 plane for top/bottom reflector region axially.
- *Time step*: Improved quasi-static model with auto time step was used for transient problem, predictor-corrector method was used to decide time steps.

4. **Bibliographical references for the code.**

5. **Cross-section library used.**

Given 2G nodal library.

6. **Other assumptions and comments useful for interpreting correctly the results. Provide short description of the T-H solution.**

- Cross-section interpolation for TFU and moderator density was performed independently, so only the following data points were used:

(TFU, TMO) = (560, 752.06), (560, 711.87), (560, 661.14)
(900, 752.06)
(1320, 752.06)

- T-H solution based on two-phase, constant pressure of 15.5 MPa.

1. **Name and address of participant(s).**

Hyun Chul Lee, lhc@kaeri.re.kr
Jae Woon Yoo, jwyoo@kaeri.re.kr
Jae Man Noh, jmnoh@kaeri.re.kr
Hyung Kook Joo, hkjoo@kaeri.re.kr

2. **Establishment(s).**

Nuclear Reactor Engineering Department, Korea Atomic Energy Research Institute

3. **Name of code system(s) and computational method, angular and spatial approximation used.**

- *Code*: NUREC v1.1, 2G nodal method, AFEN kernel.
- *Radial discretisation*: 4 nodes/FA.
- *Axial discretisation*: 20 equidistant planes in the active fuel region, 1 plane for the top reflector, 1 plane of the bottom reflector.
- *Time discretisation*: Crank-Nicolson with 2-10 ms time step (time step size is determined automatically).

4. **Bibliographical references for the code.**

Yoo, J.W., Jae Man Noh, Hyung Kook Joo, "Development of MOX Fuelled Core Analysis Code Based on the Refined Analytic Function Expansion Nodal Method", *Proceedings of Korean Nuclear Society Autumn Meeting*, Yongpyong, Korea, October 2003.

Lee, H.C., J. W. Yoo, Jae Man Noh, Hyung Kook Joo, "Benchmark Analysis of the NUREC Code with OECD/NEA and US NRC PWR MOX/UO_2 Control Rod Ejection Problem", *Proceedings of Korean Nuclear Society Autumn Meeting*, Yongpyong, Korea, October 2004.

5. **Cross-section library used.**

2G nodal library.

6. **Other assumptions and comments useful for interpreting correctly the results. Provide short description of the T-H solution.**

- Axial quantities are node average, not point values.
- Pin-power reconstruction performed only with the un-rodded form functions.

1. **Name and address of participant(s).**

Tomasz Kozlowski, tomasz@ecn.purdue.edu
Thomas J. Downar, downar@ecn.purdue.edu

2. **Establishment(s).**

Purdue University
1290 Nuclear Engineering Building
West Lafayette, IN 47906
USA

3. **Name of code system(s) and computational method, angular and spatial approximation used.**

- *Code*: PARCS v2.70:
  - 2G ANM with NEM for critical nodes (HYBRID kernel) for 2G solution;
  - multi-group NEM method (NEMMG kernel) for 4G and 8G solution.
- *Radial discretisation*: 4 nodes/FA.
- *Axial discretisation*: 20 equidistant planes in the active fuel region, 1 plane for the top reflector, 1 plane of the bottom reflector.
- *Time discretisation*: fully implicit with 2 ms time step.

4. **Bibliographical references for the code.**

Downar, Thomas J., *et al*., "PARCS: Purdue Advanced Reactor Core Simulator", *PHYSOR 2002*, Seoul, Korea, 7-10 Oct. (2002).

5. **Cross-section library used.**

2G nodal library for the 2G solution, 4G and 8G nodal library for the MG solution.

6. **Other assumptions and comments useful for interpreting correctly the results. Provide short description of the T-H solution.**

- Axial quantities are node average, not point values.
- T-H solution based on 1-D mass-energy equations, no momentum, one-phase, constant mass flow rate, constant pressure of 15.5 MPa.
- 2G pin-power reconstruction performed only with the un-rodded form functions.
- No pin-power available for NEMMG kernel.
- UO_2 conductivity [Eq. (3) in specifications] was used for all fuel types.

1. **Name and address of participant(s).**

   Akiko Takeuchi, takeuchi-akiko@jnes.go.jp
   Tetsuo Nakajima, nakajima-tetsuo@jnes.go.jp

2. **Establishment(s).**

   Japan Nuclear Energy Safety Organisation (JNES), Safety Analysis and Evaluation Division

3. **Name of code system(s) and computational method, angular and spatial approximation used.**

   SKETCH-INS, multi-group nodal method, 4 nodes/FA.
   TRAC-P with 1 ms time step was used for the transient.

4. **Bibliographical references for the code.**

   Nakajima, T., *et al*., "Analysis of the PWR MSLB Benchmark Using the Coupled 3-D Neutronics and Thermal-hydraulic Code SKETCH-INS/TRAC-P", *NUTHOS-6*, Nara, Japan, 4-8 October 2004.

5. **Cross-section library used.**

   2G nodal library.

6. **Other assumptions and comments useful for interpreting correctly the results. Provide short description of the T-H solution.**

   - Axial quantities are node average.
   - T-H solution performed using two-phase flow model in three dimensions (r-z-θ).
   - Pin-power reconstruction performed with the un-rodded and rodded form functions and then only with the un-rodded form functions for Part I of the benchmark.

1. **Name and address of participant(s).**

Sergey Akimushkin, akimushkin@nsi.kiae.ru
Alexander Avvakumov, avvakumov@nsi.kiae.ru
Valery Malofeev, malofeev@nsi.kiae.ru
Victor Sidorov, sidorov@nsi.kiae.ru

2. **Establishment(s).**

Russian Research Center "Kurchatov Institute", Nuclear Safety Institute

3. **Name of code system(s) and computational method, angular and spatial approximation used.**

- *Code*: BARS, advanced method of heterogeneous reactor theory, 5G (prompt) and 6G (delayed), axial representation of neutron flux is based on Fourier series expansion, quasi-static approach in dynamics calculation.
- *Radial discretisation*: pin-by-pin.
- *Axial discretisation*: no discretisation within the core; formally to represent calculational results 24 zones in the active fuel region and 2 zones for the top and bottom reflectors were used.
- *Time discretisation*: from 0.005 s (min.) to 0.1 s (max.) depending on power behaviour.

4. **Bibliographical references for the code.**

Avvakumov, A., V. Malofeev, "Validation of an Advanced Heterogeneous Model for LWR Detailed Pin-by-pin Calculations", *Proceedings of the International Conference on the Physics of Nuclear Science and Technology*, USA, October 1998.

Avvakumov, A., V. Malofeev, V. Sidorov, *Analysis of Pin-by-pin Effects for LWR Rod Ejection Accident*, NUREG/IA-0175, NSI RRC KI 90-12/1-3-00, IPSN/00-13, March 2000.

Akimushkin, S., A. Avvakumov, V. Malofeev, A. Roslyakov, "Validation of a Pin-by-pin Heterogeneous Method Against LWR MOX Benchmarks", *Proc. of the International Conference on the New Frontiers of Nuclear Technology: Reactor Physics, Safety and High-performance Computing (PHYSOR 2002)*, Korea, October 2002.

5. **Cross-section library used. If own library was used, please describe homogenisation method, number of groups and data reduction method.**

5G library of lambda-matrices (instead of cross-sections) generated with the physics lattice code UNK using ENDF/B-VI.

6. **Other assumptions and comments useful for interpreting correctly the results. Provide short description of the T-H solution.**

- Axial quantities are zone average, not point values.
- T-H solution based on the RELAP5/mod 3.2 calculations (assembly averaged T-H parameters).

1. **Name and address of participant(s).**

Han-Gyu Joo, joohan@snu.ac.kr
Jin-Young Cho, jyoung@kaeri.re.kr
Kang-Seog Kim, kimks@kaeri.re.kr

2. Establishment(s).

Seoul National University, Nuclear Engineering Department, Seoul, Korea
Korea Atomic Energy Research Institute, Daejeon, Korea

3. Name of code system(s) and computational method, angular and spatial approximation used.

- *Code*: DeCART v1.10, method of characteristics within the CMFD framework.
- *Angular discretisation*: 4 azimuthal angles per 90°, 2 polar angles per 90°.
- *Spatial discretisation*: 0.04 cm average ray spacing, 3 radial rings in the fuel, 1 moderator ring around the cladding. The spatial mesh for fuel cell flat flux regions is shown in the figure below (gap and IFBA were neglected on the figure for clarity).

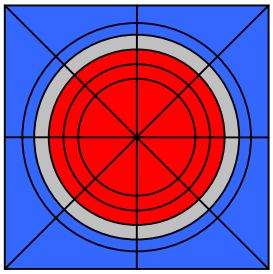

4. **Bibliographical references for the code.**

Joo, H.G., J.Y. Cho, Y. Kim, "Dynamic Implementation of the Equivalence Theory in the Heterogeneous Whole Core Transport Calculation", *PHYSOR 2002*, Seoul, Korea, 7-10 Oct. (2002).

5. **Cross-section library used. If own library was used, please describe homogenisation method, number of groups and data reduction method.**

47G library based on HELIOS v1.8 library, transport-corrected P0 scattering, subgroup method for resonance calculation.

6. **Other assumptions and comments useful for interpreting correctly the results. Provide short description of the T-H solution.**

Currently only solution for Part I of the benchmark is available.

1. **Name and address of participant(s).**

Armin Seubert, armin.seubert@grs.de
Winfried Zwermann, winfried.zwermann@grs.de
Siegfried Langenbuch, siegfried.langenbuch@grs.de

2. **Establishment(s).**

Gesellschaft für Anlagen- und Reaktorsicherheit (GRS) mbH
Forschungsinstitute
D-85748 Garching
Germany

3. **Name of code system(s) and computational method, angular and spatial approximation used.**

- *Code*: DORT 3.2 (Discrete Ordinates Oak Ridge Neutron/Photon Transport Code). DORT is part of the DOORS code system developed at Oak Ridge National Laboratory and solves the two-dimensional multi-group transport equation for neutral particles in discrete ordinates representation for both rectangular and curvilinear geometry.

  The submitted DORT solution of Part I.a of the benchmark has been calculated for 1/4 of the core with pin-cell homogenised cross-sections in 16 energy groups and P1 scattering order.

- *Angular discretisation*: level-symmetric S4 quadrature.

- *Spatial discretisation*: rectangular geometry with 2 spatial meshes per pin cell in each spatial dimension (in total: 4 nodes per pin cell).

4. **Bibliographical references for the code.**

Rhoades, W.A., R.L. Childs, “The DORT Two-dimensional Discrete Ordinates Transport Code”, *Nuclear Science & Engineering*, 99, 1, pp. 88-89 (May 1988).

5. **Cross-section library used. If own library was used, please describe homogenisation method, number of groups and data reduction method.**

- *Burn-up calculation*: 190 group library based on HELIOS v1.8 library.

- *DORT transport calculation*: pin-cell homogenised macroscopic cross-sections in 16 energy groups and P1 scattering order.

6. **Other assumptions and comments useful for interpreting correctly the results. Provide short description of the T-H solution.**

Currently, only the solution for Part I.a of the benchmark is available.

1. Name and address of participant(s).

Andrey Myasnikov, myasnikov@nsi.kiae.ru

2. Establishment(s).

Russian Research Center, "Kurchatov Institute"

3. Name of code system(s) and computational method, angular and spatial approximation used.

MCNP-4C2

4. Bibliographical references for the code.

MCNP4C2 – Monte Carlo N-particle Transport Code System, LANL, RSICC Computer Code Collection, CCC-701 (June 2001).

5. Cross-section library used. If own library was used, please describe homogenisation method, number of groups and data reduction method.

ENDF/B-VI (with last available revisions); processed with NJOY.

6. Other assumptions and comments useful for interpreting correctly the results. Provide short description of the T-H solution.

Only partial solution for Part I of the benchmark is available.

Type of calculation:	Criticality
Number of cycles:	9 800
Number of histories per cycle:	5 000
Number of cycles to be skipped:	400

LIST OF CONTRIBUTORS

Authors

Tomasz Kozlowski (Purdue University, USA, currently at KTH, Sweden)
Thomas J. Downar (Purdue University, USA)
Enrico Sartori (OECD/NEA)

Problem specifications

Tomasz Kozlowski (Purdue University, USA, currently at KTH, Sweden)
Thomas J. Downar (Purdue University, USA)
Enrico Sartori (OECD/NEA)

Benchmark participants

Tomasz Kozlowski (Purdue University, USA, currently at KTH, Sweden)
Siegfried Langenbuch (GRS, Germany)
Armin Seubert (GRS, Germany)
Winfried Zwermann (GRS, Germany)
Tetsuo Nakajima (JNES, Japan)
Akiko Takeuchi (JNES, Japan)
Toshikazu Takeda (Osaka University, Japan)
Sho Tanaka (Osaka University, Japan)
Jin-Young Cho (KAERI, Korea)
Hyung Kook Joo (KAERI, Korea)
Kang-Seog Kim (KAERI, Korea)
Hyun Chul Lee (KAERI, Korea)
Jae Man Noh (KAERI, Korea)
Jae Woon Yoo (KAERI, Korea)
Han-Gyu Joo (SNU, Korea)
Sergey Akimushkin (Kurchatov Institute, Russia)
Alexander Avvakumov (Kurchatov Institute, Russia)
Valery Malofeev (Kurchatov Institute, Russia)
Andrey Myasnikov (Kurchatov Institute, Russia)
Victor Sidorov (Kurchatov Institute, Russia)
Hakim Ferroukhi (PSI, Switzerland)
Martin Zimmermann (PSI, Switzerland)
Thomas J. Downar (Purdue University, USA)